1981

The crystal and molecular structures of selected organic and organometallic compounds and an algorithm for empirical absorption correction

Barbara Ann Karcher
Iowa State University

INFORMATION TO USERS

This was produced from a copy of a document sent to us for microfilming. While the most advanced technological means to photograph and reproduce this document have been used, the quality is heavily dependent upon the quality of the material submitted.

The following explanation of techniques is provided to help you understand markings or notations which may appear on this reproduction.

1. The sign or "target" for pages apparently lacking from the document photographed is "Missing Page(s)". If it was possible to obtain the missing page(s) or section, they are spliced into the film along with adjacent pages. This may have necessitated cutting through an image and duplicating adjacent pages to assure you of complete continuity.

2. When an image on the film is obliterated with a round black mark it is an indication that the film inspector noticed either blurred copy because of movement during exposure, or duplicate copy. Unless we meant to delete copyrighted materials that should not have been filmed, you will find a good image of the page in the adjacent frame. If copyrighted materials were deleted you will find a target note listing the pages in the adjacent frame.

3. When a map, drawing or chart, etc., is part of the material being photographed the photographer has followed a definite method in "sectioning" the material. It is customary to begin filming at the upper left hand corner of a large sheet and to continue from left to right in equal sections with small overlaps. If necessary, sectioning is continued again—beginning below the first row and continuing on until complete.

4. For any illustrations that cannot be reproduced satisfactorily by xerography, photographic prints can be purchased at additional cost and tipped into your xerographic copy. Requests can be made to our Dissertations Customer Services Department.

5. Some pages in any document may have indistinct print. In all cases we have filmed the best available copy.

University
Microfilms
International

300 N. ZEEB RD., ANN ARBOR, MI 48106

KARCHER, BARBARA ANN

THE CRYSTAL AND MOLECULAR STRUCTURES OF SELECTED ORGANIC AND ORGANOMETALLIC COMPOUNDS AND AN ALGORITHM FOR EMPIRICAL ABSORPTION CORRECTION

Iowa State University

PH.D. 1981

The crystal and molecular structures of selected organic and organometallic compounds and an algorithm for empirical absorption correction

by

Barbara Ann Karcher

A Dissertation Submitted to the
Graduate Faculty in Partial Fulfillment of the
Requirements for the Degree of
DOCTOR OF PHILOSOPHY

Department: Chemistry
Major: Physical Chemistry

Approved:

Signature was redacted for privacy.

In Charge of Major Work

Signature was redacted for privacy.

For the Major Department

Signature was redacted for privacy.

For the Graduate College

Iowa State University
Ames, Iowa

1981

TABLE OF CONTENTS

GENERAL INTRODUCTION

This dissertation reports the single crystal X-ray structure determinations of four compounds. These were done to provide structural confirmations and other information at the molecular level which would help explain their observed properties.

Many thioketones are unstable and polymerize rapidly, but they can be stabilized by coordination to metals. In order to characterize accurately this coordination, $Cr(CO)_5(S{=}CMe_2)$ was investigated by single crystal X-ray diffractometery.

The conformation of the nitrogen atoms in rigid tris(dialkylamino)-phosphine could be either planar or pyramidal. The crystal and molecular structure of $PSN_3C_6H_{12}$ was determined to resolve this ambiguity. A new data collection method, which was utilized in the X-ray diffraction analysis of this compound, is also discussed in this dissertation.

A large number of structurally different complexes can be formed using large diisonitrile ligands. These include dimers with metal-metal bonds and complexes with metal atoms bridged by these bidentate ligands. Since very little structural data are available on such complexes, the structure of $RhO_4N_4C_{72}BH_{76}\cdot 1.5\ NC_2H_3$ was determined.

Two forms of the phosphorinane ligand exist -- one with the phosphorus lone pair axial and the other with the pair equatorial. The structure determination of $MoP_2O_{10}C_{16}H_{22}$ was carried out to ascertain whether or not there is retention of conformation at the phosphorus in complexes containing this ligand.

This dissertation also includes an empirical absorption correction program, which provides an easy and relatively inexpensive way to correct intensity data for absorption effects. A complete listing and discussion of the program are included.

Explanation of Dissertation Format

In this dissertation, the crystal and molecular structures of each compound are discussed in separate sections. Each section constitutes an adaptation of a journal article which either has been published or is in preparation, with the exception of the section on the absorption correction program which is not an adaptation of a journal article. The appendix contains a published communication to which some supplemental information in tabular form has been added. All tables, figures, and references are numbered consecutively throughout this dissertation.

THE CRYSTAL AND MOLECULAR STRUCTURE OF $Cr(CO)_5(SCMe_2)$, A THIOKETONE COMPLEX

Introduction

Few metal complexes of thioketones have been reported since most thioketones are unstable and polymerize rapidly. Gingerich and Angelici have succeeded in preparing complexes of the type $M(CO)_5(S{=}CR_2)$ in which the thioketone was stabilized by coordination to the metal atom, where M=Cr, Mo, or W, and R=Me, Et or Ph (1). In order to characterize more accurately the coordination of a thioketone to a metal, a single crystal X-ray investigation of $Cr(CO)_5(S{=}CMe_2)$ was carried out.

Experimental

Crystal Data $CrSO_5C_8H_6$, M.W. = 266.19, monoclinic $P2_1/a$, $\underline{a}$ = 10.468(8), $\underline{b}$ = 11.879(5), $\underline{c}$ = 9.575(6) Å, β = 108.14(9)°, V = 1131.50 $Å^3$, ρ_c = 1.562 $g.cm^{-3}$, Z = 4, μ = 12.38 cm^{-1} (Mo K_α, λ = 0.70954 Å).

Crystals were obtained from R. J. Angelici and a nearly spherical crystal of diameter 0.2 mm was wedged into a Lindeman glass capillary and mounted on a four-circle diffractometer. Initial ω-oscillation photographs were taken and these verified that the crystal was indeed single. Fourteen reflections were selected from these photographs and their approximate positions were input into an automatic indexing program (2). The reduced cell and reduced cell scalars that resulted indicated monoclinic symmetry. Subsequent ω-oscillation Polaroid photographs taken around each of the three cell axes in turn verified the 2/m Laue symmetry

as well as the reciprocal lattice spacings predicted by the program.

Accurate unit cell parameters and their standard deviations were obtained by a least-squares fit to the $\pm 2\theta$ values of eleven independent high angle reflections measured on a previously aligned four-circle diffractometer.

Collection and Reduction of X-ray Intensity Data Data were collected at room temperature using an automated four-circle diffractometer designed and built in the Ames Laboratory and previously described by Rohrbaugh and Jacobson (3). The diffractometer is interfaced to a PDP-15 computer in a real-time mode and is equipped with a scintillation counter. Graphite reflected-beam monochromated Mo K_α radiation (λ = 0.70954 Å) was used for data collection. Within a sphere of $2\theta \leq 50°$ ($\sin\theta/\lambda = 0.595$ $Å^{-1}$), all data in the hkl and $hk\bar{l}$ octants were measured using an ω-stepscan technique.

As a general check on crystal and electronic stability, the intensities of three standard reflections were remeasured every 75 reflections. These standard reflections were not observed to vary to any significant degree during the entire period of data collection. In all, 2224 reflections were recorded in this manner. Examination of the data revealed the following systematic absences: $h0\ell$ when $h = 2n+1$ and $0k0$ when $k = 2n+1$. These absences uniquely determine the space group as $P2_1/a$.

The intensity data were corrected for Lorentz and polarization effects, but absorption corrections were not deemed necessary; the maximum and minimum transmission factors were 0.906 and 0.862,

respectively. The estimated variance in each intensity was calculated by

$$\sigma_I^2 = C_T + 2C_B + (0.03\ C_T)^2 + (0.03\ C_B)^2,$$

where C_T and C_B represent the total and background counts and the factor 0.03 represents an estimate of non-statistical errors. The estimated deviations in the structure factors were calculated by the finite difference method (4). After correction, 1435 reflections with $I_o > 3\sigma_{Io}$ were retained for use in the structure solution and refinement. During the latter stages of the investigation it was discovered that six large reflections suffered from secondary extinction effects. These effects were corrected via the approximation $I_o' = I_o x(1+gI_c)$, where an average value for g, 1.9315×10^{-5}, was determined using the ten largest I_o's.

Solution and Refinement

The position of the chromium atom was obtained from an analysis of a sharpened three-dimensional Patterson function. All other non-hydrogen atoms were found by successive structure factor (5) and electron density map calculations (6). Analysis of an electron density difference map also revealed some small residual electron density near the carbon. Therefore, methyl hydrogen atoms were added such as to complete the tetrahedron around the carbon and best fit the residual electron density. The C-H distances were set equal to 1.0 Å, and all isotropic thermal parameters for hydrogen were fixed at 4.0 $Å^2$.

Refinement of the positional and anisotropic thermal parameters (Table 1) for all non-hydrogens by a full-matrix least-squares procedure minimizing the function $\Sigma\omega(|Fo|-|Fc|)^2$, where $\omega = 1/\sigma_F^2$, yielded a final

Table 1. Final atomic positional[a] and thermal parameters[b] for $Cr(CO)_5(SCMe)_2$

(a) Positional parameters

Atom	x	y	z
Cr	0.2979(1)[c]	0.1103(1)	0.1765(1)
S	0.1753(2)	0.0848(2)	0.3455(2)
C1	0.1303(9)	0.1160(6)	0.0245(9)
O1	0.0337(7)	0.1181(5)	-0.0737(7)
C2	0.2981(8)	-0.0485(7)	0.1661(8)
O2	0.3012(7)	-0.1456(5)	0.1579(7)
C3	0.4706(10)	0.1026(7)	0.3187(10)
O3	0.5753(7)	0.0957(6)	0.4002(9)
C4	0.2997(9)	0.2706(7)	0.1891(9)
O4	0.2988(8)	0.3662(6)	0.1941(8)
C5	0.3821(10)	0.0343(10)	0.0343(10)
O5	0.4331(9)	0.1233(6)	-0.0553(9)
C6	0.2247(9)	0.1431(6)	0.5061(8)
C7	0.1516(13)	0.1162(9)	0.6146(12)
C8	0.3385(12)	0.2217(10)	0.5605(11)
H17	0.1191	0.1867	0.6480
H27	0.2128	0.0750	0.7002
H37	0.0720	0.0665	0.5652
H48	0.3077	0.3005	0.5437
H58	0.3836	0.2086	0.6689
H68	0.4068	0.2063	0.5079

[a]In this table and subsequent atomic parameter tables, the positional parameters for all atoms are represented in fractional unit cell coordinates.

[b]The β_{ij} are defined by: $T = \exp\{-(h^2\beta_{11} + k^2\beta_{22} + \ell^2\beta_{33} + 2hk\beta_{12} + 2h\ell\beta_{13} + 2k\ell\beta_{23})\}$. If only the β_{11} column is listed, this corresponds to an isotropic temperature factor.

[c]In all tables, the values in parentheses denote the estimated standard deviations in the last digits.

Table 1 (Continued) (b) Thermal parameters

	Atomic Temperature Factors x 10^2					
Atom	β_{11}	β_{22}	β_{33}	β_{12}	β_{13}	β_{23}
Cr	1.22(2)	0.66(1)	1.18(2)	-0.02(1)	0.24(1)	0.04(1)
S	1.37(3)	0.87(2)	1.30(3)	-0.10(2)	0.33(2)	-0.14(2)
C1	1.5(1)	0.82(6)	1.4(1)	0.05(7)	0.33(9)	0.06(7)
O1	1.52(9)	1.35(7)	1.9(1)	-0.09(6)	-0.04(8)	0.17(6)
C2	1.3(1)	0.85(7)	1.4(1)	0.02(7)	0.57(8)	0.05(6)
O2	2.3(1)	0.77(5)	2.4(1)	0.05(6)	0.7(1)	0.00(6)
C3	1.4(1)	0.91(7)	1.8(1)	-0.04(7)	0.3(1)	0.03(7)
O3	1.24(8)	1.71(8)	2.6(1)	0.09(6)	0.00(9)	0.17(8)
C4	1.5(1)	0.82(7)	1.51(1)	0.02(7)	0.34(9)	-0.08(7)
O4	3.1(2)	0.84(6)	2.6(1)	-0.19(7)	0.6(1)	-0.06(6)
C5	1.9(1)	0.92(7)	1.6(1)	0.03(8)	0.6(1)	0.31(7)
O5	2.3(1)	1.47(8)	2.2(1)	0.18(7)	1.1(1)	0.38(7)
C6	1.3(1)	0.80(6)	1.4(1)	0.18(7)	0.31(9)	0.02(6)
C7	1.9(2)	1.07(9)	1.9(2)	-0.12(10)	0.7(1)	-0.16(9)
C8	1.5(2)	1.3(1)	1.7(2)	-0.3(1)	0.2(1)	-0.2(1)
H17	400					
H27	400					
H37	400					
H48	400					
H58	400					
H68	400					

crystallographic discrepancy factor, $R = \Sigma||Fo|-|Fc||/\Sigma|Fo|$, of 0.075. The final weighted discrepancy factor $R_\omega = \{\Sigma\omega(|Fo|-|Fc|)^2/\Sigma\omega|Fo|^2\}^{1/2}$, was 0.11 The scattering factors of Hanson et al. (7) were used for all non-hydrogen atoms. The chromium scattering factors were modified for anomalous dispersion effects (8). Hydrogen scattering factors were those of Stewart et al. (9).

Description of the Structure and Discussion

A computer-generated perspective drawing (10) of $Cr(CO)_5(SCMe_2)$ is shown in Figure 1, and the more important bond distances and angles are given in Tables 2 and 3, respectively.

The coordination around the chromium is basically octahedral, the C-Cr-C angles ranging from 88.5(3) to 90.9(3)°. The sulfur atom, however, is slightly displaced from the octahedral position, forming S-Cr-C angles of 85.3(3), 87.8(3), 94.6(3), and 95.8(4)° with C2, C1, C4, and C3, respectively. This distortion appears to be due to a steric effect arising from repulsion between the C8 methyl group and the adjacent carbonyl groups, the shortest contacts being 3.357 Å and 3.584 Å (Table 2).

The Cr-C distance trans to the Me_2CS group is significantly shorter, 1.835(12) Å, than the remaining Cr-C distances (averaging 1.898(8) Å). Such a shortening has been observed in other metal carbonyl complexes when a CO group is trans to a poorly π-bonding ligand and can be attributed to a resultant increase in the π-bonding of the CO.

The Cr-C equatorial distances compare quite well with those previously reported, namely: 1.90 Å in $(MeSCN)Cr(CO)_5$ (11), 1.88 Å in

$(C_6H_5)_3PCr(CO)_5$ (12), and 1.903 Å in $Me_3PSCr(CO)_5$ (13).

The C-O distances are all essentially equal to within three standard deviations, averaging 1.146 Å. The C=S distance 1.618(8) Å, is significantly shorter than the 1.71 Å distance found in ethylene thiourea and thioacetamide, but longer than the 1.561 Å distance in HNCS (14).

Least-squares planes and deviations from these planes are given in Table 4. As can be seen from this table, the Me_2CS group shows no significant deviation from planarity and the chromium atom also essentially lies in this plane. This would be in accord with a model which assumes sp^2 hybridization at the sulfur and interaction between the sulfur and the chromium via a lone pair in one of these hybrids. The Cr-S-C6 angle of 120.8(4)° is also in excellent agreement with such a model. In addition, this plane approximately bisects the angle between the planes formed by S, Cr, C3, C4, C5 and S, Cr, C1, C3, C5, indicating rotation about the Cr-S bond to minimize repulsive effects.

Unit cell packing is illustrated in Figure 2 and no abnormally short contacts are present; the shortest intermolecular distance being 3.270 Å between O1 and C5 in adjacent molecules.

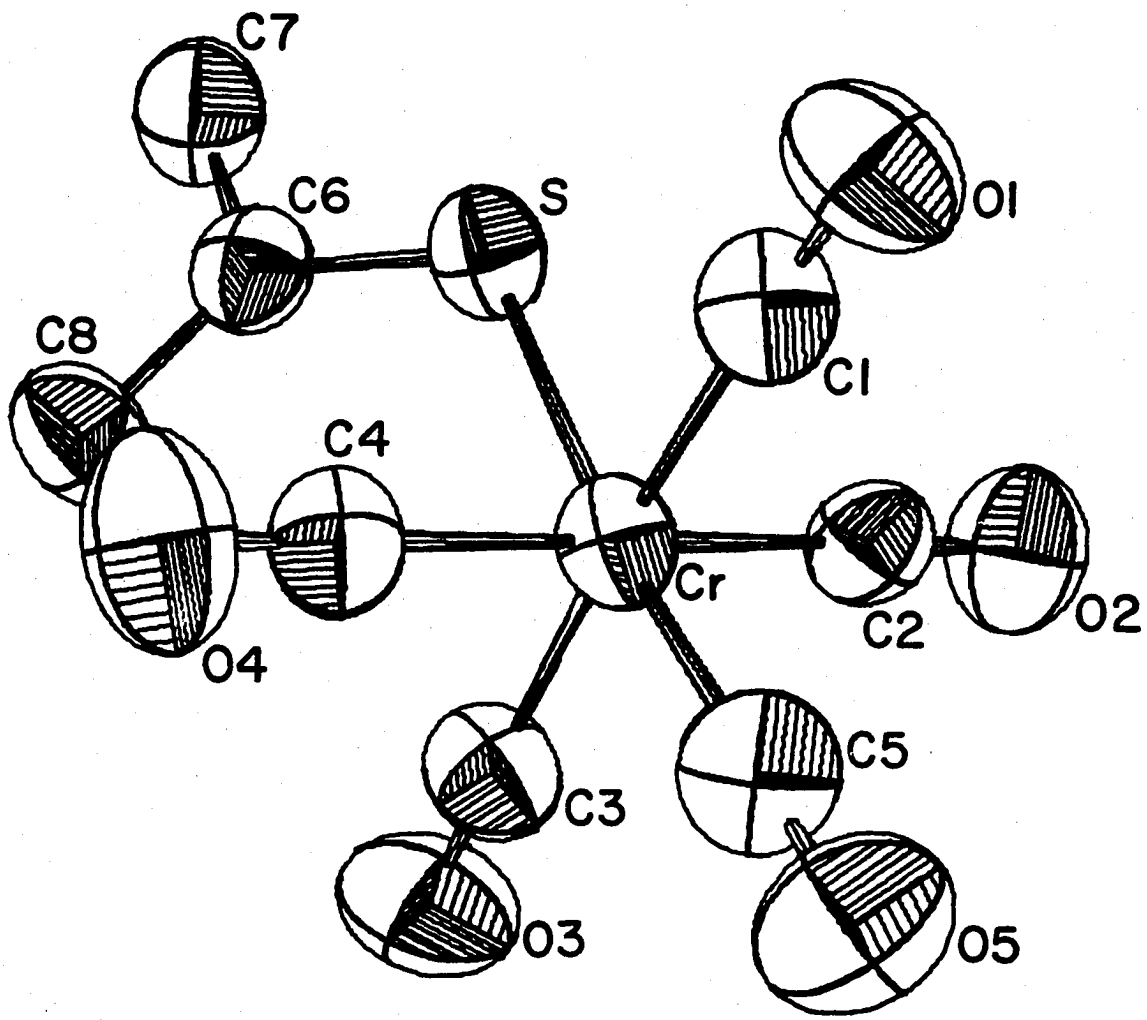

Figure 1. A computer-generated perspective drawing of $Cr(CO)_5(SCMe_2)$, excluding the hydrogen atoms

Table 2. Selected bond distances (Å)

Cr-S	2.377(4)	C6-C8	1.477(14)
Cr-C1	1.901(8)	C4-C8	3.584(15)
Cr-C2	1.889(8)	O4-C8	3.809(15)
Cr-C3	1.896(9)	C3-C8	3.357(17)
Cr-C4	1.905(8)	O3-C8	3.621(17)
Cr-C5	1.835(12)	O1-O1[a]	3.314
C1-O1	1.147(10)	O1-O2[a]	3.359
C2-O2	1.156(11)	C1-O2[b]	3.516
C3-O3	1.132(11)	O1-O2[b]	3.519
C4-O4	1.146(11)	C5-O1[c]	3.270
C5-O5	1.153(16)	C5-O4[c]	3.831
S-C6	1.618(8)	O1[b]-C1[c]	3.377
C6-C7	1.497(17)	O1[b]-O1[c]	3.314

[a]Via symmetry operation $(\bar{x},\bar{y},\bar{z})$.

[b]Via symmetry operation $(\frac{1}{2}-x,\frac{1}{2}+y,\bar{z})$.

[c]Via symmetry operation $(\frac{1}{2}+x,\frac{1}{2}-y,z)$.

Table 3. Selected angles (°)

S-Cr-C1	87.8(3)	O4-C4-Cr	178.7(8)
S-Cr-C2	85.3(3)	O5-C5-Cr	179.4(13)
S-Cr-C3	95.8(4)	C6-S-Cr	120.8(4)
S-Cr-C4	94.6(3)	C7-C6-C8	114.7(8)
S-Cr-C5	173.9(2)	C1-Cr-C2	90.6(3)
O1-C1-Cr	175.5(10)	C1-Cr-C4	90.1(3)
O2-C2-Cr	178.0(10)	C2-Cr-C3	88.7(3)
O3-C3-Cr	177.5(10)	C2-Cr-C4	90.9(3)

Table 4. Equations of least squares planes[a] and interplanar angles

Atom	Distance from Plane (Å)	Atom	Distance from Plane (Å)
	Plane I fitting Cr-C1-C2-C3-C4		
	0.7090 X + 0.02899 Y - 0.70671 Z - 0.77433 = 0		
Cr	-0.0390	C3	0.0225
C1	0.0224	C4	-0.0027
C2	-0.0027		
	Plane II fitting Cr-S-C3-C4-C5		
	0.067599 X + -0.02144 Y + 0.73659 Z - 2.87378 = 0		
Cr	0.0339	C4	0.0219
S	-0.0351	C5	-0.0463
C2	0.0256		
	Plane III fitting Cr-S-C1-C3-C5		
	-0.04078 X + 0.99424 Y + 0.09909 Z - 1.31559 = 0		
Cr	0.0408	C3	0.0202
S	-0.0361	C5	-0.0483
C1	0.0234		
	Plane IV fitting S-C6-C7-C8		
	0.53567 X - 0.76966 Y + 0.34737 Z - 0.74726 = 0		
S	0.0015	C8	0.0016
C6	-0.0046	Cr	0.1908
C7	0.0014		
	Plane V fitting Cr-S-C2-C4		
	0.65649 X - 0.02119 Y + 0.75403 Z - 2.87810 = 0		
Cr	0.0074	C2	-0.0036
S	-0.0001	C4	-0.0036

Interplanar Angles

Plane	Plane	Angle (°)
I	II	87.51
I	III	85.98
I	IV	83.63
I	V	86.02
II	III	88.61
II	IV	50.61
III	IV	41.17

[a]Planes are defined as $c_1X + c_2Y + c_3Z = d$, where X, Y, and Z are cartesian coordinates which are related to the triclinic cell coordinates (x,y,z) by the transformations $X = xz \sin\gamma + zc\,(\cos\beta\cos\alpha\cos\gamma)\sin\gamma$, $Y = xa\cos\gamma + yb + zc\cos\alpha$, and $Z = zc(1 - \cos^2\alpha - \cos^2\beta - \cos^2\gamma + 2\cos\alpha\cos\beta\cos\gamma)^{\frac{1}{2}}/\sin\gamma$.

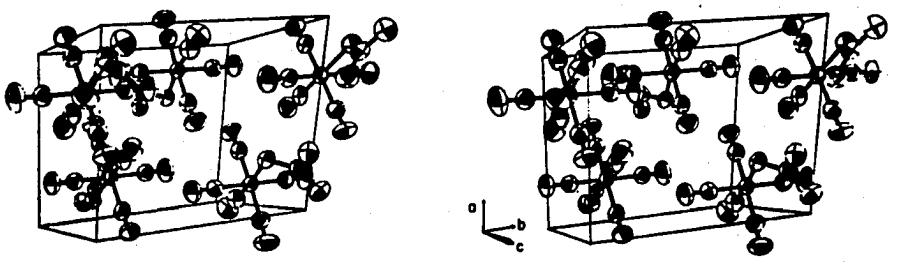

Figure 2. Unit cell stereograph of $Cr(CO)_5(SCMe_2)$

EVALUATION OF A NEW DATA COLLECTION METHOD PRIMARILY EMPLOYING UNFILTERED RADIATION: THE CRYSTAL AND MOLECULAR STRUCTURE OF $PSN_3C_6H_{12}$, A TRIS(DIALKYLAMINO)PHOSPHINE WITH PYRAMIDAL NITROGENS

Introduction

The conformational preference of acyclic tris(dialkylamino)phosphine is uncertain due to a lack of unambiguous structural and photoelectron spectroscopy (PES) data (15). Generally, X-ray diffraction studies have shown nitrogen to be planar or nearly so in compounds containing the groups PN<, O=PN<, or S=P-N< (16). However, steric effects can cause a deviation from this planarity, such as in tris(morpholino) and tris(piperdino)phosphine (17). The rigid tris(dialkylamino)phosphine 1 was synthesized (18) to duplicate closely the C_{3v} structure which has been proposed to be the dominant conformer of $P(NMe_2)_3$ (19).

Unlike $P(NMe_2)_3$,

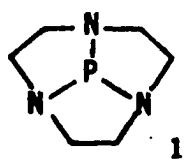

1

1 is unstable with respect to formation of a polymer-like material on standing. However, as has been demonstrated in Professor Verkade's group, sulfur readily adds to 1 and forms a more stable crystalline solid; therefore, a single crystal X-ray diffraction study to characterize accurately the molecular structure of this compound was undertaken.

Because this molecule does not contain any atoms of large atomic number, copper radiation appeared to be the best choice for data collection. This also gave the opportunity to use the Hilger-Watts

diffractometer in a previously untried data collection mode, i.e. using a method designed to yield maximum intensities available from the X-ray tube.

To produce a good set of data, it is necessary to eliminate the effect of K_β radiation to get a "pure" K_α source. K_β radiation is one of the characteristic lines in an X-ray spectrum (Figure 3). It occurs when K electrons are knocked from their orbitals and M shell electrons fill the vacancies. The M shell electrons' decrease in potential energy appears as K_β radiation. K_α radiation, which is produced by L to K electron transitions, is usually three to six times more intense than K_β. Thus, the K_α lines are the most useful for determining structures. However, unless precautionary measures are taken, the K_β radiation will contribute to the diffracted intensities and interfere with the interpretation of the diffraction pattern.

This can be done by a filter which absorbs the K_β radiation more than the K_α. Like many other absorption processes, the ratio of the final to the initial intensity $(\frac{I}{I_o})$ is $e^{-\mu t}$, where μ is the linear absorption coefficient and t is the path length through the absorber. The absorption coefficient for a given element increases with increasing wavelength until the energy of the incident X-ray is no longer able to knock an electron out of its orbital. At this point there is a sudden drop in μ (an absorption edge), before it starts again increasing with λ (Figure 4). The K absorption edge for nickel metal occurs between the K_β and K_α peaks of copper radiation, making it a suitable filter for removing CuK_β radiation. To obtain a CuK_β/K_α intensity ratio of 1/100,

Figure 3. X-ray spectrum with characteristic peaks for copper radiation

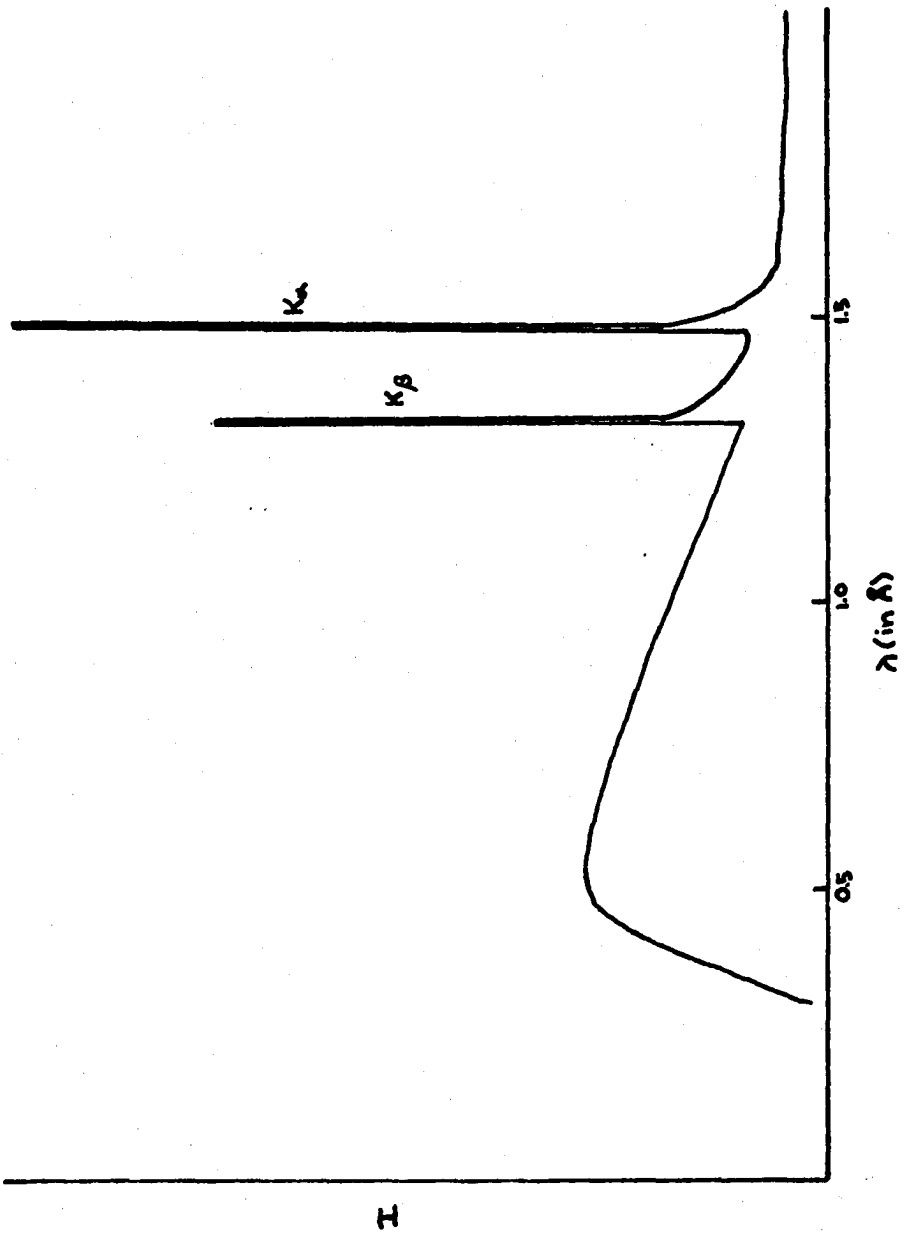
Kα
Kβ
1.5
1.0
0.5
λ (in Å)
I

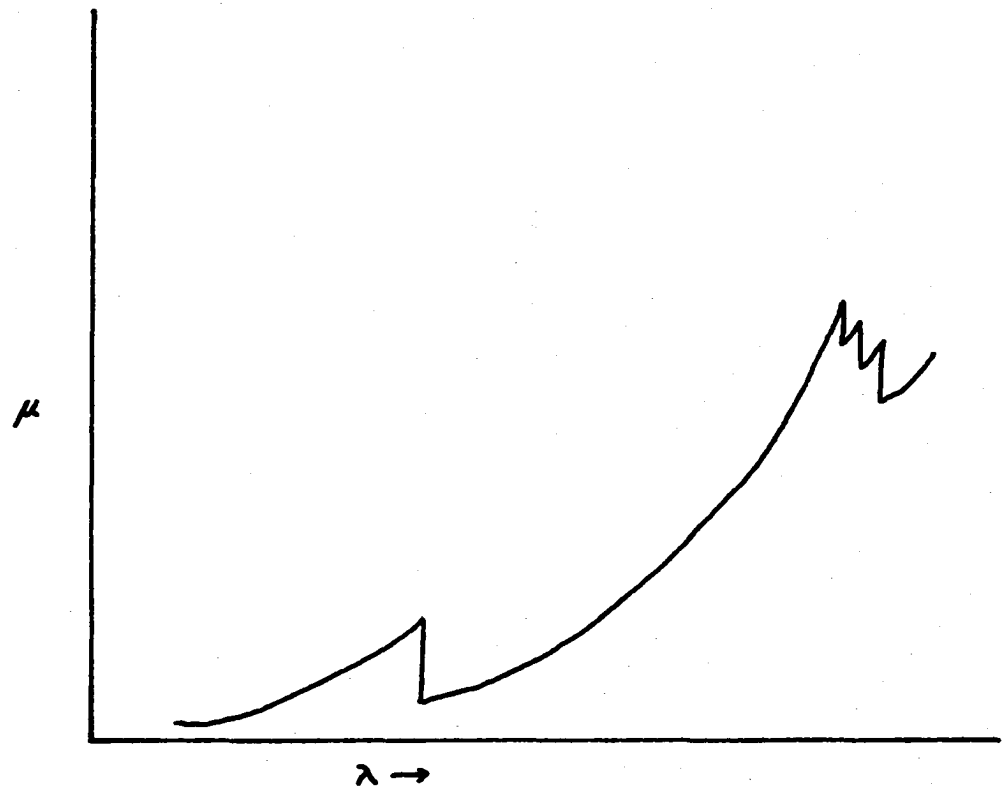

Figure 4. μ as a function of λ

a nickel thickness of 0.015 mm is needed. However, the K_α intensity is also reduced to 55% of its original value (20). Since the error in intensity measurement is related to $\sqrt{I}$, this decrease in intensity increases the errors in the data set.

From Bragg's law, $\lambda = 2d\sin\theta$, it is evident that diffraction peaks from K_β radiation occur closer to the origin of diffraction space, i.e. at smaller θ values, than their K_α counterparts; therefore, it was decided to try using unfiltered copper radiation for most of the data collection and filtered radiation for reflections which would have a β peak within 1.5° in theta from them. Counting times would be appropriately adjusted. Since the Hilger-Watts diffractometer allowed the user to insert automatically a filter material if desired, the whole process could be executed under computer control.

Experimental

Crystal Data $PSN_3C_6H_{12}$, MW = 189.0, monoclinic, $P2_1/n$, $\underline{a}$ = 10.896(1), $\underline{b}$ = 11.443(1), $\underline{c}$ = 7.288(1) Å, β = 104.45(1)°, V = 880.0 Å^3, ρ_{calc} = 1.43 g/cm^3, Z = 4, μ = 43.85 cm^{-1} (Cu K_α, λ = 1.5418 Å).

A sample of the material was obtained from D. H. White and J. G. Verkade. An approximately spherical crystal (0.15 mm diameter) was then mounted in a Lindeman glass capillary.

Initial ω-oscillation photographs verified the crystal was single. The approximate positions of eleven reflections selected from these pictures were input into an autoindexing program (2). The resultant reduced cell and reduced cell scalars indicated monoclinic symmetry.

Accurate unit cell parameters and their standard deviations were obtained by a least-squares fit to the ±2θ values of eleven independent high angle reflections measured on a previously aligned four-circle diffractometer.

Collection and Reduction of X-Ray Intensity Data Data collection was done at room temperature utilizing a fully automated Hilger-Watts four-circle diffractometer equipped with a scintillation counter and interfaced through an SDS-910 computer to a PDP-15 computer in a real time mode. Data were collected (Cu K_α radiation, λ = 1.5418 Å) using a θ-2θ scan technique with a β-filter inserted only when a β peak was calculated to make a contribution within the scan range. Counting times were increased to keep the intensities comparable.

To determine when α and β peaks will overlap, the d-spacing for a reflection is calculated using the wavelength of K_α radiation. The theta angle for a β peak with this d-spacing is equal to $\sin^{-1}\left(\frac{n\lambda_{CuK_\beta}}{2d}\right)$, where n is the order of the reflection. Theta values are calculated starting with n=1. n is incremented by 1 until a theta (β) value is within 1.5 degrees of the theta value of the K_α reflection, the theta (β) is greater than theta (α) + 1.5°, or the arcsine argument is greater than 1. If the first condition occurs, a flag is returned to the calling routine which causes the β-filter to be inserted and the counting time increased for the reflection in question. A listing of the subroutine is given in Table 5.

All data (2274 reflections) within a sphere of 2θ≤100° in the hkl, $hk\bar{l}$, $h\bar{k}l$, and $h\bar{k}\bar{l}$ octants were measured. Of these, only 151 required

Table 5. The subroutine for calculating when a beta filter is necessary

```
BETA:  PROCEDURE (CTRL);
/* CTRL CONTAINS THE PARAMETERS PASSED FROM THE CALLING ROUTINE SUCH AS
H, K, L AND THE ANGLE SETTINGS FOR THE GIVEN REFLECTION */
        DECLARE 1 CTRL,
                  2 XTAL (9,8)   FIXED,    2 ORNT (3,3)   FLOAT,
                  2 DMIN         FLOAT,    2 DMAX -       FLOAT,
                  2 RFLX (12)    FIXED,    2 MODE (50)    FIXED,
                  2 SCRA (62)    FIXED,    2 FSCR (9)     FLOAT;
DCL THETA FLOAT,HLONG FLOAT,J FIXED, BPEAK FLOAT, N FIXED, AH FIXED,
 AK FIXED, AL FIXED, MIN FIXED, I FIXED;
/* SET THE FLAG VARIABLE SO THAT THE FILTER IS NOT INSERTED */
MODE(3)=0;
THETA=RFLX(4)/200.0;
AH=ABS(RFLX(1));
AK=ABS(RFLX(2));
AL=ABS(RFLX(3));
/* DETERMINES THE ORDER OF THE CURRENT REFLECTION */
MIN=AH;
IF ((AK<MIN)&(AK^=0))|(MIN=0) THEN MIN=AK;
IF ((AL<MIN)&(AL^=0))|(MIN=0) THEN MIN=AL;
DO I=MIN TO 1 BY -1;
IF (MOD(AH,I)=0)&(MOD(AK,I)=0)&(MOD(AL,I)=0) THEN DO ;
N=I;
GO TO LONG;
END;
END;
/* HLONG IS 1/D=SPACING FOR LAMBDA K=ALPHA */
LONG: HLONG=2.0*SIN(THETA*0.017453)/(N*1.5418);
/* CALCULATE THE THETA VALUE FOR VARIOUS ORDERS OF BETA PEAKS WITH
D=SPACING HLONG */
J=0;
ANGLE: J=J+1;
BPEAK=1.3922*J*HLONG*0.5;
IF BPEAK>=1.0 THEN RETURN;
BPEAK=ASIN(BPEAK)*57.29578;
IF (THETA+1.5)<BPEAK THEN RETURN;
IF BPEAK<(THETA-1.5) THEN GO TO ANGLE;
/* THE BETA PEAK IS WITHIN THE SCAN RANGE THE FLAG VARIABLE IS SET
SO THAT THE FILTER WILL BE INSERTED AND THE COUNTING TIME INCREASED */
MODE(3)=1000;
RETURN;
END BETA;
```

the β-filter to be inserted.

The intensities of three standard reflections were remeasured after every 75 reflections to check on crystal and electronic stability. These standard reflections did not vary significantly during the entire data collection period. Examination of the data revealed the following systematic absences: hOℓ when h+ℓ = 2n+1 and OkO when k = 2n+1. Thus, the space group was determined to be $P2_1/n$.

The intensity data were corrected for Lorentz and polarization effects. Calculated transmission factors ranged from 0.29 to 0.42; hence, no absorption corrections were made. The estimated variance in each intensity was calculated by

$$\sigma_I^2 = C_T + K_t C_B + (0.03\ C_T)^2 + (0.03\ C_B)^2,$$

where C_T, C_B, and K_t represent the total counts, background counts, and a counting-time constant, respectively, and the factor 0.03 represents an estimate of non-statistical errors. The estimated deviations in the structure factors were calculated by the finite difference method (4). Observed data (2085 reflections with $|F_o| > 3\sigma F_o$) were averaged and the 887 independent reflections that resulted were then used in the structure solution and refinement.

Solution and Refinement

The direct methods program MULTAN (21) was used to determine the positions of all non-hydrogen atoms. These atoms were then refined using a full-matrix least-squares procedure minimizing the function $\Sigma\omega(|F_o|-|F_c|)^2$ with $\omega = 1/\sigma_F^2$ (5). After all non-hydrogen atoms were

refined anisotropically, hydrogen positions were calculated with a C-H bond length of 1.05 Å, and an H-C-H bond angle of 109.5°. The isotropic temperature factors for these hydrogens were set equal to 6.0 $Å^2$; these factors as well as their positional parameters were not refined. An analysis of the weights, ω, was performed via the requirement that $\omega(|Fo|-|Fc|)^2$ should be a constant function of $|Fo|$ and $\sin\theta/\lambda$ (22). Reflections at very low or very high $\sin\theta/\lambda$ were somewhat overweighted; therefore, all ω's were subsequently adjusted. Refinement converged to a crystallographic residual index, $R = \{\Sigma_i||F_i^{obsd}|-|F_i^{calc}||\}\Sigma_i|F_i^{obsd}| = 0.058$. Its weighted counterpart, $R_\omega = \{(\Sigma\omega_i(F_i^{obsd}-F_i^{calc})^2]/\Sigma_i\omega_2|F_i^{obsd}|^2\}^{1/2}$, where $\omega_i = 1/\sigma_{F_i}^2$, was 6.9%. The scatt ing factors of Hanson et al. (7) were used for all non-hydrogens, with ose for the phosphorus and sulfur atoms modified for the real and imaginary part of anomalous dispersion (8). The hydrogen atoms' scattering factors were those of Stewart et al. (9).

The final positional and thermal parameters are listed in Table 6. The standard deviations were calculated from the inverse matrix of the final least-squares refinement cycles. Bond distances and angles are given in Table 7. Computer generated perspective drawings of one of the molecules and the unit cell are shown in Figures 5 and 6.

Discussion

Strain in $PSN_3C_6H_{12}$ forces the nitrogens into a pyramidal configuration, with average bond angles of 109°. This agrees quite well with the 109.8° average in tris(morpholino)phosphine (2) and 111.5° in tris(piperidino)phosphine (3) (17). In contrast, the NPN angles

Table 6. Final atomic positional and thermal parameters for $PSN_3C_6H_{12}$

(a) Positional parameters

Atom	x	y	z
P	0.2030(1)	0.1475(1)	-0.0554(2)
S	0.3221(1)	0.0471(1)	0.1103(2)
N1	0.0703(4)	0.1853(3)	0.0086(5)
N2	0.2542(4)	0.2813(3)	-0.1026(6)
N3	0.1396(4)	0.0998(3)	-0.2768(6)
C1	0.0901(5)	0.3111(5)	0.0602(8)
C2	0.1591(5)	0.3675(4)	-0.0737(8)
C3	0.2639(6)	0.2702(5)	-0.3006(9)
C4	0.1546(6)	0.1956(5)	-0.4075(8)
C5	0.0058(5)	0.0714(4)	-0.2772(7)
C6	-0.0390(5)	0.1619(4)	-0.1561(8)
H1-C1	0.002	0.3522	0.0472
H2-C1	0.1448	0.3188	0.2004
H1-C2	0.0950	0.3871	-0.2034
H2-C2	0.2043	0.4445	-0.0137
H1-C3	0.2591	0.3533	-0.3632
H2-C3	0.3502	0.2303	-0.3033
H1-C4	0.0713	0.2457	-0.4455
H2-C4	0.1749	0.1609	-0.5300
H1-C5	-0.0515	0.0743	-0.4167
H2-C5	0.0012	-0.0124	-0.2205
H1-C6	-0.0661	0.2389	-0.2341
H2-C6	-0.1161	0.1292	-0.1094

Table 6 (Continued) (b) Thermal parameters[a]

Atom	Atomic Temperature Factors x 10^3					
	β_{11}	β_{22}	β_{33}	β_{12}	β_{13}	β_{23}
P	6.4(1)	4.4(1)	18.7(3)	-0.5(1)	1.9(1)	1.4(1)
S	11.0(2)	5.9(1)	36.9(5)	-0.5(1)	-5.4(2)	4.5(2)
N1	9.3(4)	6.4(3)	18.9(9)	-2.4(3)	5.4(5)	-1.4(4)
N2	7.6(4)	5.5(3)	26(1)	-0.4(3)	4.4(5)	2.7(4)
N3	8.6(4)	6.6(3)	22(1)	0.2(3)	4.8(5)	-0.1(6)
C1	11.3(6)	7.2(5)	28(1)	-1.9(4)	7.1(7)	-4.1(6)
C2	8.6(5)	4.8(4)	31(1)	-1.0(4)	5.0(7)	-0.4(6)
C3	12.8(7)	9.7(5)	34(2)	-0.1(5)	12.4(9)	3.4(7)
C4	15.9(7)	10.0(5)	22(1)	-0.5(5)	9.3(8)	1.2(7)
C5	9.4(5)	6.7(4)	24(1)	-1.2(4)	2.5(6)	-1.7(6)
C6	8.8(5)	8.6(5)	29(1)	-0.9(4)	3.7(7)	-2.0(6)

[a]The isotropic temperature factors for all hydrogen atoms were set equal to 6.0 $Å^2$.

Table 7. Intramolecular bond distances and angles

Distances (Å)		Angles (°)	
P-S	1.919(2)	S-P-N1	118.2(2)
P-N1	1.682(4)	S-P-N2	117.6(1)
P-N2	1.694(4)	S-P-N3	117.4(2)
P-N3	1.680(4)	N1-P-N2	100.0(2)
N1-C1	1.490(7)	N1-P-N3	100.0(2)
N1-C6	1.489(6)	N2-P-N3	100.1(2)
N2-C2	1.483(6)	N1-C1-C2	108.2(4)
N2-C3	1.478(8)	N1-C6-C5	106.4(4)
N3-C4	1.488(7)	N2-C2-C1	106.5(4)
N3-C5	1.494(7)	N2-C3-C4	108.2(5)
C1-C2	1.517(8)	N3-C4-C3	106.5(4)
C3-C4	1.514(8)	N3-C5-C6	107.8(4)
C5-C6	1.518(8)	C1-N1-C6	114.4(4)
		C2-N2-C3	114.7(4)
		C4-N3-C5	115.0(4)

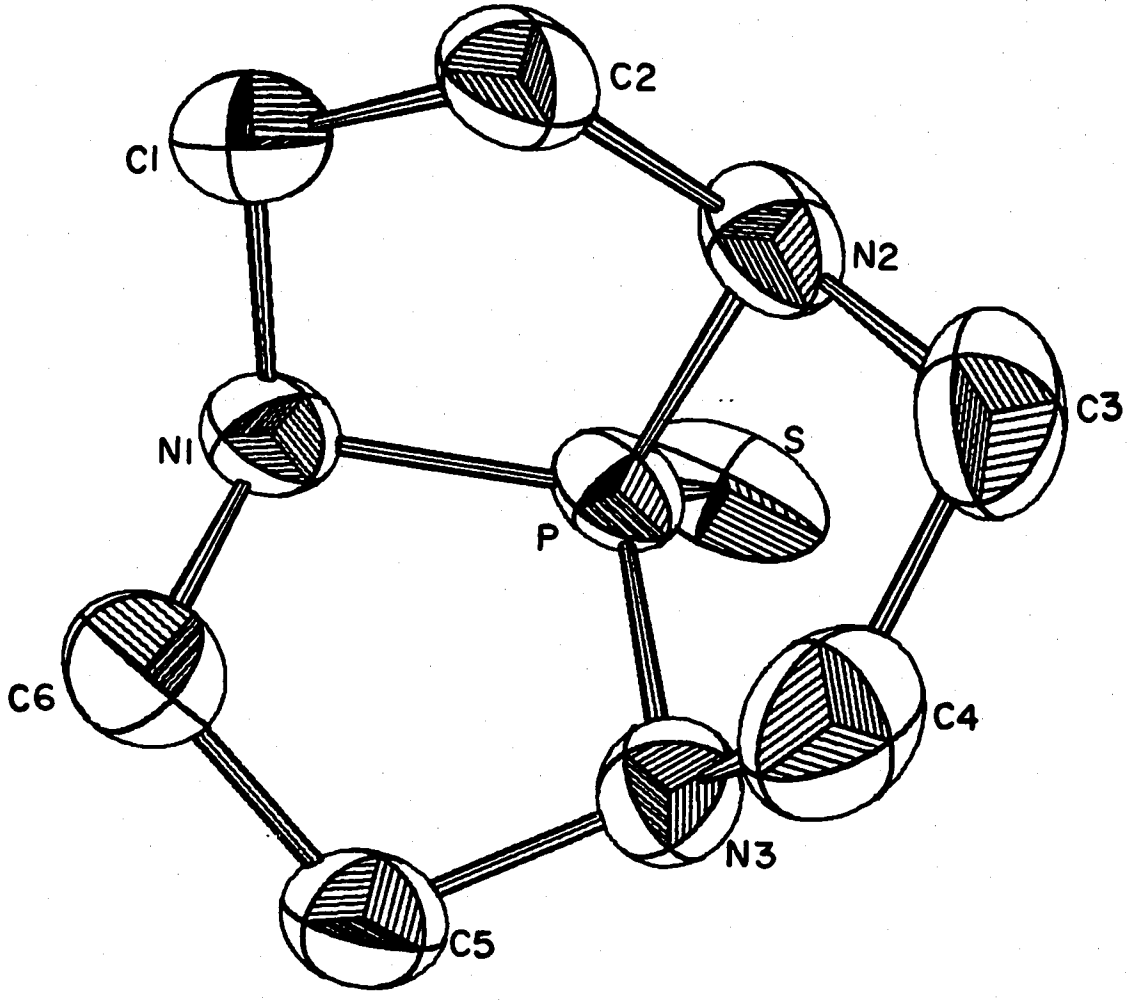

Figure 5. A computer-generated drawing of $PSN_3C_6H_{12}$, excluding the hydrogen atoms

Figure 6. Unit cell stereograph of $PSN_3C_6H_{12}$

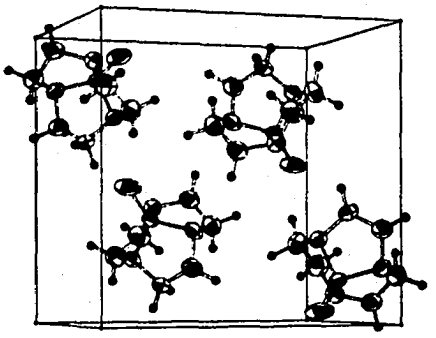

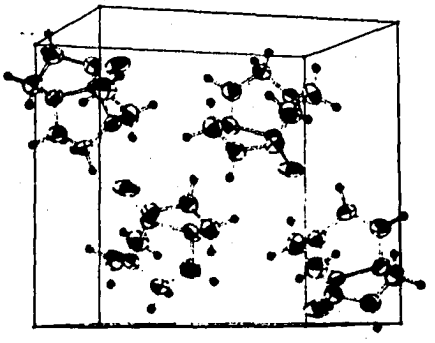

(101° average) remain near those encountered in isomeric $SP(\overline{NCH_2(CH_2)_3}$ (100°) (23). These angles average 102° in 2 and 101.6° in 3. Both compounds 2 and 3 have two P-N distances, 1.73 and 1.69 Å (average). The shorter of these distances is comparable to the 1.685 Å average observed in this structure. The C-N and C-C distances compare similarly in these three compounds. The P=S bond length of 1.919 Å in $PSN_3C_6H_{12}$ is in agreement with those in amidithion (1.908 Å) (24) and leptophos (1.911 Å) (25).

Each of the five-membered rings in this structure contains a carbon atom (C2, C4 and C6 in Figure 5) which is puckered away from the sulfur and out of the nearly planar arrays of the remaining ring atoms. This produces an average dihedral angle of 11.6° in the S-P-N-&p on the N system.

Using radiation which was filtered only when necessary worked quite well. Initially, a set of data with completely unfiltered copper radiation was collected. It refined to an agreement factor of 8.2%. Eliminating from the data set those reflections which were determined to have a β contribution reduced the R factor to 7.6%. The agreement factor was improved to 5.9% with the occasionally filtered radiation. The consistency of identical, non-symmetry related bond distances and angles is excellent, also indicating that good data can be collected in this manner. For example, the P-N distances [1.682(4), 1.694(4), and 1.680(4) Å] and the N-P-N angles [100.0(2), 100.0(2), and 100.1(2)°] are all identical within three standard deviations. Thus, filtering the radiation only when an α and a β peak will overlap, produces a better

data set without significantly increasing the time required for data collection. It should also be emphasized that in only a small percentage of the time (6.6%) was a filter even necessary. This percentage is fairly constant for a given type of radiation. For example, an orthorhombic 15 x 18 x 20 Å cell, whose reciprocal lattice is considerably more closely spaced than the title compound's lattice, was calculated to require a filter for 6.8% of the reflections for copper radiation. (There are also many more sparsely populated diagonals in such a lattice.) This same cell using molybdenum radiation ($\lambda \cong 0.71$ Å) would require a β filter for 20.2% of the data. A smaller 10 x 11 x 7 Å crystal would require a filter 22.3% of the time using Mo radiation. Since molybdenum radiation produces a more closely spaced reciprocal lattice than copper radiation, this increase in overlap of the α and β lattices would be expected.

THE CRYSTAL AND MOLECULAR STRUCTURE OF $RhO_4N_4C_{72}BH_{76}\cdot 1.5NC_2H_3$, A METAL COMPLEX WITH DIISONITRILE LIGANDS

Introduction

Dimeric rhodium(I)-diisocyano ligand complexes of the form $Rh_2(\text{diisocyanide})_2X_2$ have been reported (26-31). In these compounds, X = Cl, BF_4, PF_6 or BPh_4 and the diisocyanides contain three to six-member carbon chains, dimethylcyclohexane, or dimethylbenzene. In solution, these complexes can aggregate to form oligomers (32); the extent of this oligomerization is dependent, in part, on the steric nature of the ligand.

Angelici and co-workers have synthesized larger bidentate isonitrile ligands (33) and have prepared numerous metal complexes with them. Since these ligands are larger, there exists a much larger number of structurally different complexes that could be formed including moities where two rhodium atoms are bridged by the bidentate ligand. Very little accurate structural data were available on such complexes. Thus, the crystal and molecular structure determination of $RhO_4N_4C_{72}BH_{76}\cdot 1.5NC_2H_3$ was carried out to obtain firm structural information on the ligand's interactions within Rh(I) complexes of this type.

Experimental

Crystal Data $RhO_4N_4C_{72}BH_{76}\cdot 1.5NC_2H_3$, M.W. = 1235.2, triclinic, $P\bar{1}$, a = 17.355(8), b = 21.135(10), c = 10.757(5) Å, α = 101.29(5), β = 98.36(5), γ = 113.92(4)°, V = 3424.15 $Å^3$, ρ_c = 1.22 $g\cdot cm^{-3}$, Z = 2, μ = 3.33 cm^{-1} (Mo K_α, λ = 0.71034 Å).

A red prismatic crystal with approximate dimensions 0.4 x 0.2 x 0.15 mm was selected for data collection from a sample kindly supplied by Drs. Mark Winzenburg and R. J. Angelici. The crystal was then mounted in a Lindeman glass capillary and glued in place with Duco cement.

Initial ω-oscillation photographs verified the crystal was single. From these pictures, 15 reflections were chosen as input for an auto-indexing procedure (2). The resulting cell scalars indicated triclinic symmetry. The absence of mirror symmetry and the predicted reciprocal lattice spacings were confirmed by ω-oscillation photographs about each axis.

Fifteen high-angle reflections were used to obtain accurate cell parameters and their standard deviations. A least-squares fit was done on their ±2θ values, which were measured on an aligned four-circle diffractometer.

Collection and Reduction of Intensity Data Room temperature data were collected using the Ames Laboratory fully automated four-circle diffractometer (3). Backgrounds were measured by offsetting 0.75° in ω. Scans were done by beginning at the calculated peak center and stepping until the minimum of the two background values, measured as noted above, was reached. Counting times were 1.0 second per 0.01° step in ω. All

data within a 2θ sphere of 45° were measured with reflected-beam graphite monochromated Mo K_α radiation (λ = 0.71034 Å). A total of 10,257 reflections were collected in the hkl, $\bar{h}\bar{k}l$, $\bar{h}k\bar{l}$, and $h\bar{k}\bar{l}$ octants using an ω-stepscan technique.

Initially, four reflections were remeasured after every 75 reflections as a check on crystal and electronic stability. These standards decayed considerably during the first portion of data collection in which 675 reflections were measured. After this period, the crystal stabilized; this was indicated by three standards whose intensities no longer varied appreciably during the completion of data collection. The fourth standard was eliminated after 675 reflections, because its intensity was too low for good statistics. The decay, based on the integrated intensities of three standards, was fit to a quadratic polynomial: $y(x) = 0.7027 + 0.0008421\ x + 0.0000001495\ x^2$, where x is the reflection number and y(x) is a multiplier for the intensity of each reflection. The first portion of the data was scaled down in this manner. During the total period of data collection, a decay in these standards of 35% was noted.

A Howells, Phillips, and Rogers test (34) indicated the structure has a center of symmetry. Thus, the space group was assumed to be $P\bar{1}$. The data were corrected for Lorentz and polarization effects. Each intensity's variance was calculated by

$$\sigma_I^2 = C_T + k_B C_B + (0.03\ C_T)^2 + (0.03\ C_B)^2,$$

where C_T, C_B and k_B are the total count, background count, and a counting time factor, respectively, and the 0.03 factor is an estimate of

non-statistical errors. The finite difference method (4) was used to compute the estimated deviations in the structure factors. A reflection was considered observed if $I > 3\sigma_I$; after equivalent data were averaged, there were 5912 reflections which met this requirement.

The calculated minimum and maximum transmittances are 0.88 and 0.95, respectively. In light of the relatively high transmission and the small (3.8%) deviation from the average, no absorption correction was made.

Solution and Refinement

The position of the rhodium atom was determined by the analysis of a sharpened Patterson function. A single superposition was then done shifting by the rhodium-rhodium vector. From the resultant map most of the non-hydrogen atoms were found. Their positions were put into a block diagonal structure factor least-squares program (35); a sharpened electron density map (36) based on this refinement readily revealed the positions of the remaining non-hydrogens. Electron density difference maps were then used to locate hydrogen atoms. Several groups of methyl hydrogens were not found on these maps probably due to low barriers to rotation; hence, they were not input into the refinement. The thermal parameters for the hydrogens were set equal to 4.0 $\AA^2$; neither the thermal nor the positional parameters were varied in refinement.

The block-matrix least-squares minimized the function $\Sigma\omega(|Fo|-|Fc|)^2$, where $\omega = 1/\sigma_F{}^2$. The function $\omega(|Fo|-|Fc|)^2$ should be a constant with respect to $|Fo|$ and $\sin\theta/\lambda$ (22). An analysis of the weights (ω) indicated some overweighting at very low and very high $\sin\theta/\lambda$ values; these values were subsequently adjusted. The conventional agreement factor,

$R = \Sigma||Fo|-|Fc||/\Sigma|Fo|$, was equal to 8.1%.

The difference map still had two large peaks near the origin. Their maxima were about 1.14 Å apart. The peak nearest the origin, where there is an inversion center, was 1.45 Å from its symmetry-related partner. These peaks were resolved as a disordered acetonitrile molecule -- acetonitrile was used as a solvent in the crystal preparation. The nitrogen sits at x,y,z half the time and $\bar{x},\bar{y},\bar{z}$ the remainder of the time. The positions of the methyl carbon and the sp hybridized carbon are inversion related; the position of the nitrogen at any given time distinguishes them.

After this group was input and refined, a final residual index of 7.0% resulted. The weighted residual $R_\omega = (\Sigma\omega(Fo-Fc)^2/\Sigma\omega Fo^2)^{1/2}$, was equal to 7.9%. The scattering factors used in the refinement were those of Hanson *et al.* (7); the rhodium factors were modified for anomalous dispersion effects (8). The hydrogen scattering factors of Stewart *et al.* (9) were used.

Discussion

Figures 7 and 8 are computer generated drawings of the cation and the unit cell, respectively. Atomic parameters are found in Table 8; bond distances and angles are given in Tables 9 and 10.

The structural analysis of this complex showed that the two rhodium atoms are not bridged by the ligands and there are no strong metal-metal interactions.

Since the ligand could adopt an essentially planar configuration, it is also of interest to ascertain whether the complexes themselves pack

Figure 7. The rhodium complex cation

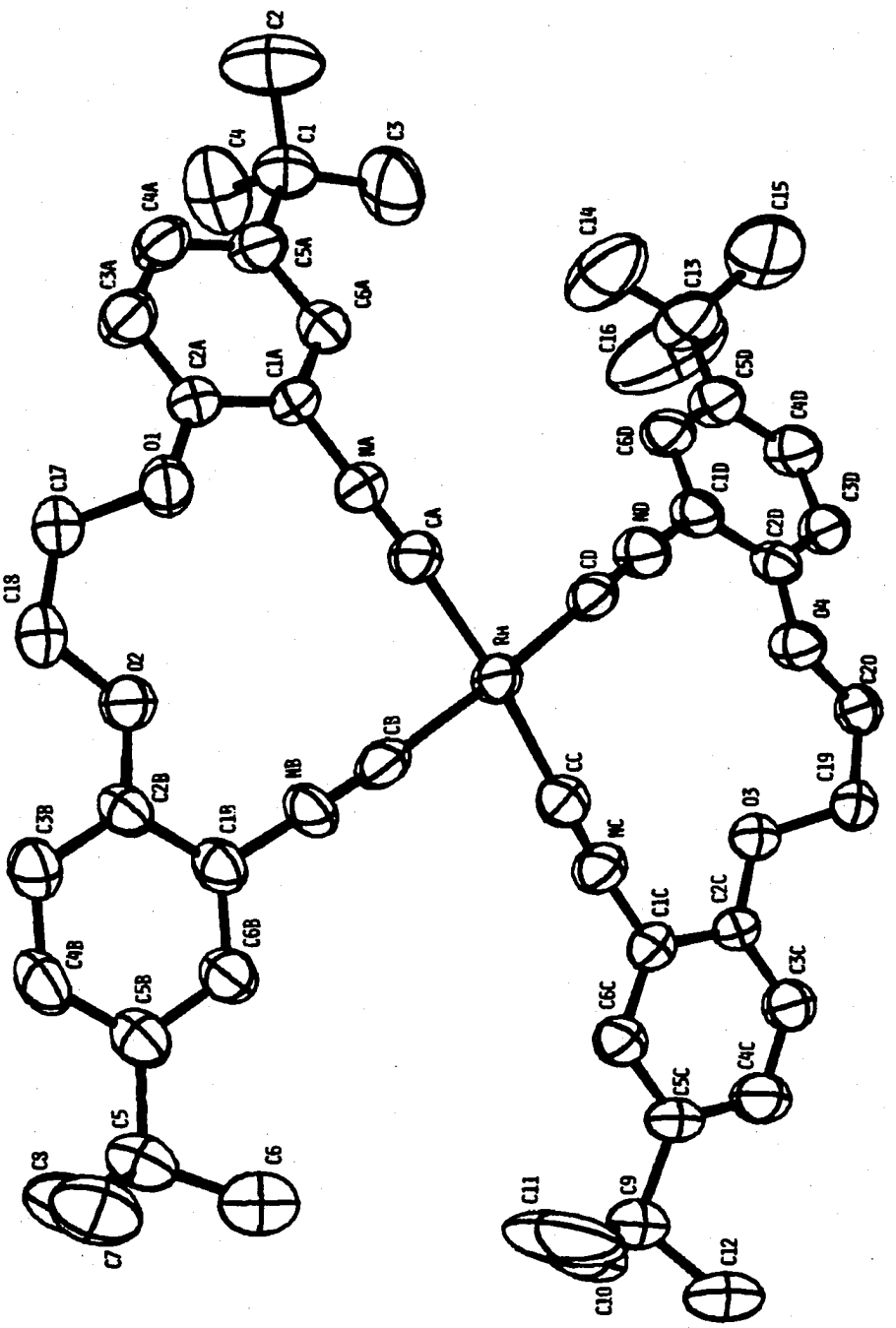
C2
C4
C1
C3
C4A
C5A
C3A
C6A
C2A
C1A
O1
NA
C17
C18
O2
C4
NB
C2B
C1B
C3B
C6B
C4B
C5B
C5
C8
C7
C6
Rh
CA
CB
CC
CD
ND
NC
C14
C15
C13
C16
C5D
C4D
C6D
C1D
C3D
C2D
O4
C20
C19
O3
C1C
C2C
C3C
C6C
C4C
C5C
C9
C11
C10
C12

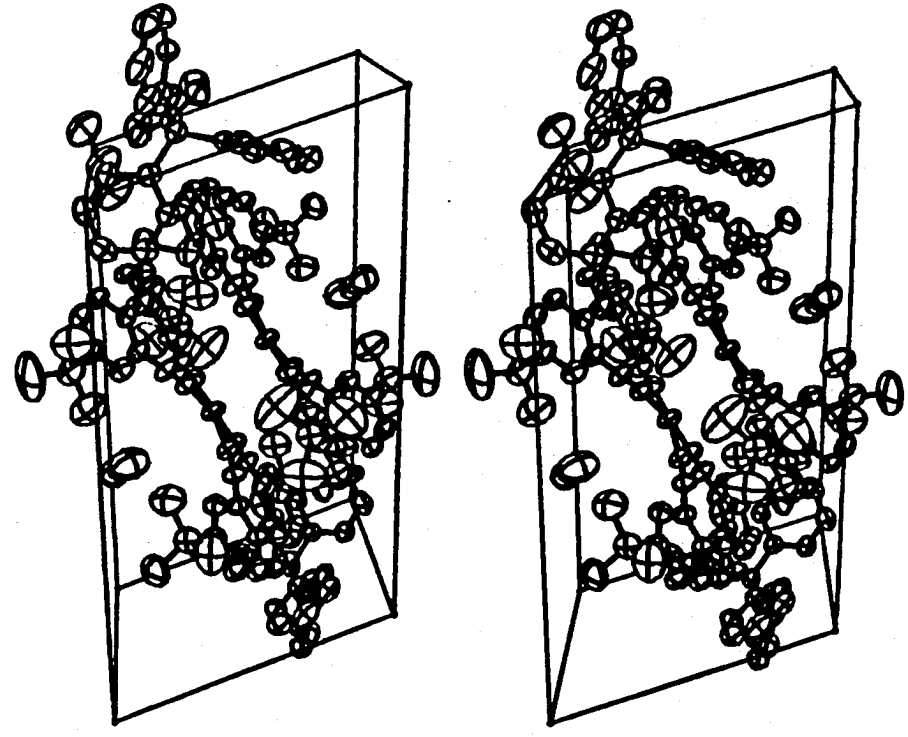

Figure 8. Unit cell stereograph of $RhO_4N_4C_{72}BH_{76} \cdot 1.5NC_2H_3$

Table 8. Final atomic positional and thermal parameters for $RhO_4N_4C_{72}BH_{76}\cdot 1.5NC_2H_3$

(a) Final positional parameters for the cation

Atom	x	y	z
Rh	0.54634(4)	0.54525(3)	0.03962(7)
CA	0.6716(4)	0.6080(4)	0.4406(7)
CB	0.5320(4)	0.6314(4)	0.4733(8)
CC	0.4189(5)	0.4880(4)	0.3300(8)
CD	0.5635(4)	0.4652(4)	0.3007(7)
NA	0.7438(4)	0.6472(3)	0.4576(6)
NB	0.5268(4)	0.6833(3)	0.5157(6)
NC	0.3453(4)	0.4542(3)	0.2865(6)
ND	0.5714(4)	0.4192(3)	0.2319(6)
C1A	0.8301(4)	0.6921(4)	0.4591(7)
C2A	0.8667(4)	0.7647(4)	0.5269(7)
C3A	0.9493(5)	0.8087(4)	0.5194(8)
C4A	0.9902(5)	0.7800(4)	0.4408(8)
C5A	0.9533(5)	0.7084(4)	0.3691(8)
C6A	0.8711(5)	0.6643(4)	0.3804(8)
C1B	0.5238(5)	0.7472(4)	0.5737(7)
C2B	0.5991(4)	0.8114(4)	0.6107(7)
C3B	0.5944(5)	0.8731(4)	0.6755(8)
C4B	0.5156(6)	0.8687(4)	0.6977(8)
C5B	0.4393(5)	0.8037(4)	0.6587(8)
C6B	0.4458(5)	0.7429(4)	0.5976(7)
C1C	0.2564(4)	0.4099(4)	0.2486(7)
C2C	0.2268(4)	0.3380(4)	0.1830(7)
C3C	0.1399(5)	0.2935(4)	0.1579(8)
C4C	0.0833(5)	0.3204(4)	0.1957(9)
C5C	0.1123(5)	0.3935(4)	0.2598(8)
C6C	0.2012(5)	0.4376(4)	0.2875(8)
C1D	0.5703(5)	0.3632(4)	0.1380(7)
C2D	0.4962(4)	0.2972(4)	0.1007(7)
C3D	0.4913(5)	0.2418(4)	0.0026(7)
C4D	0.5604(5)	0.2538(4)	-0.05611(8)
C5D	0.6351(5)	0.3196(4)	-0.0208(8)
C6D	0.6388(5)	0.3741(4)	0.0792(8)
C1	-0.9987(5)	0.6802(5)	0.2774(9)
C2	1.0903(8)	0.6996(9)	0.3529(13)
C3	0.9493(8)	0.5988(6)	0.2173(13)
C4	1.0020(9)	0.7154(6)	0.1649(11)
C5	0.3537(5)	0.8031(5)	0.6792(8)
C6	0.2817(7)	0.7264(6)	0.6470(13)
C7	0.3680(7)	0.8436(6)	0.8238(9)
C8	0.3252(7)	0.8425(6)	0.5907(10)

Table 8 (Continued)

Atom	x	y	z
C9	0.0505(5)	0.4240(5)	0.2943(10)
C10	0.0159(12)	0.4424(11)	0.178(2)
C11	0.944(10)	0.4930(10)	0.402(2)
C12	-0.0265(9)	0.3691(8)	0.327(2)
C13	0.7075(6)	0.3293(5)	-0.0905(10)
C14	0.7844(9)	0.4013(8)	-0.034(2)
C15	0.6717(11)	0.318(2)	-0.232(2)
C16	0.7406(10)	0.2731(9)	-0.077(2)
C17	0.8219(5)	0.8563(4)	0.5856(8)
C18	0.7541(5)	0.8697(4)	0.64312(8)
C19	0.2838(5)	0.2519(4)	0.1664(8)
C20	0.3463(4)	0.2355(4)	0.1011(7)
O1	0.8193(3)	0.7885(2)	0.5974(5)
O2	0.6709(3)	0.8087(2)	0.5805(5)
O3	0.2864(3)	0.3175(3)	0.1424(5)
O4	0.4317(3)	0.2935(2)	0.1624(5)

(b) Final positional parameters for the anion and the solvent molecules

B	0.7328(6)	-0.0343(5)	0.2895(8)
C21	0.7754(5)	0.0186(4)	0.1998(7)
C22	0.7581(8)	-0.0063(5)	0.0651(9)
C23	0.7897(10)	0.0379(6)	-0.0123(10)
C24	0.8399(8)	0.1106(6)	0.0428(11)
C25	0.8591(7)	0.1370(5)	0.1754(9)
C26	0.8279(5)	0.0920(4)	0.2530(8)
C27	0.7905(5)	0.0062(4)	0.4445(7)
C28	0.8712(5)	0.0087(4)	0.4876(8)
C29	0.9215(6)	0.0430(4)	0.6169(8)
C30	0.8919(6)	0.0766(4)	0.7075(8)
C31	0.8143(6)	0.0771(5)	0.6687(8)
C32	0.7627(5)	0.0429(4)	0.5387(8)
C33	0.7430(5)	-0.1095(4)	0.2475(7)
C34	0.6890(6)	-0.1741(4)	0.2708(8)
C35	0.7036(8)	-0.2346(5)	0.2536(9)
C36	0.7743(8)	-0.2337(5)	0.2093(9)
C37	0.8300(7)	-0.1719(6)	0.1827(9)
C38	0.8144(6)	-0.1117(5)	0.2031(8)
C39	0.6299(5)	-0.0520(4)	0.2760(7)
C40	0.5816(6)	-0.0391(4)	0.1739(8)
C41	0.4964(6)	-0.0505(5)	0.1689(9)

Table 8 (Continued)

Atom	x	y	z
C42	0.4553(6)	-0.0744(6)	0.2630(11)
C43	0.5001(6)	-0.0887(6)	0.3596(11)
C44	0.5852(6)	-0.0776(5)	0.3669(9)
N1	0.2917(9)	0.4463(7)	0.910(2)
C45	0.3463(7)	0.4316(6)	0.9390(11)
C46	0.4104(8)	0.4123(7)	0.9693(13)
N2	0.071(2)	0.100(2)	0.073(3)
	(c) Hydrogen positional parameters		
H-C3A	0.9780	0.8735	0.5893
H-C4A	1.0500	0.8208	0.4345
H-C6A	0.8424	0.6084	0.3109
H-C3B	0.6526	0.9233	0.7042
H-C4B	0.5145	0.9171	0.7483
H-C6B	0.3874	0.6927	0.5668
H-C3C	0.1160	0.2374	01081
H-C4C	0.0162	0.2865	0.1761
H-C6C	0.2250	0.4936	0.3389
H-C3D	0.4360	0.1902	-0.0278
H-C4D	0.5551	0.2083	-0.1308
H-C6D	0.6969	0.4258	0.1078
H1-C2	0.1378	0.7542	0.3548
H2-C2	0.0922	0.6986	0.4553
H3-C2	0.1142	0.6614	0.3092
H1-C3	-0.1187	0.5790	0.2173
H2-C3	-0.0218	0.5723	0.2756
H3-C3	-0.0446	0.5830	0.1172
H1-C4	-0.0434	0.7402	0.1650
H2-C4	0.0675	0.7583	0.1796
H3-C4	-0.0169	0.6760	0.0714
H1-C6	0.2176	0.7246	0.6464
H2-C6	0.2949	0.6990	0.7202
H3-C6	0.2770	0.7931	0.5502
H1-C8	0.2799	0.8595	0.6252
H2-C8	0.2959	0.8069	0.4896
H3-C8	0.3837	0.8899	0.5891
H1-C10	-0.0478	0.4415	0.1784
H2-C10	0.0607	0.4966	0.1743
H3-C10	0.0077	0.4036	0.0851
H1-C11	0.0575	0.5213	0.4112
H2-C11	0.1603	0.5223	0.4049
H3-C11	0.0978	0.4742	0.5014

Table 8 (Continued)

Atom	x	y	z
H1-C12	-0.0786	0.3849	0.3260
H2-C12	-0.0072	0.3615	0.4221
H3-C12	-0.0519	0.3159	0.2519
H1-C14	0.7641	0.4457	0.9668
H2-C14	0.8131	0.4075	1.0672
H3-C14	0.8332	0.4096	0.9099
H1-C16	0.8082	0.2937	0.9200
H2-C16	0.7312	0.2588	1.0117
H3-C16	0.7020	0.2236	0.8381
H1-C17	0.8869	0.9003	0.6389
H2-C17	0.8130	0.8556	0.4812
H1-C18	0.7618	0.8919	0.7415
H2-C18	0.7707	0.9099	0.6007
H1-C19	0.2221	0.2104	0.1329
H2-C19	0.3019	0.2584	0.2658
H1-C20	0.3293	0.2307	0.0030
H2-C20	0.3444	0.1872	0.1081
H-C22	0.7174	-0.0637	0.0217
H-C23	0.7771	0.0173	-0.1203
H-C24	0.8639	0.1469	-0.0212
H-C25	0.8975	0.1937	0.2193
H-C26	0.8419	0.1117	0.3593
H-C28	0.8930	0.0812	0.4153
H-C29	0.9853	0.0441	0.6519
H-C30	0.9324	0.1029	0.8078
H-C31	0.7913	0.1037	0.7398
H-C32	0.6992	0.0418	0.5034
H-C34	0.6331	-0.1746	0.3063
H-C35	0.6612	-0.2832	0.2724
H-C36	0.7861	-0.2804	0.1950
H-C37	0.8859	-0.1704	0.1477
H-C38	0.8548	-0.0638	0.1806
H-C40	0.6137	-0.0202	0.1022
H-C41	0.4625	-0.0399	0.0868
H-C42	0.3895	-0.0822	0.2519
H-C43	0.4693	-0.1068	0.4318
H-C44	0.6205	-0.0881	0.4442
H1-C46	0.8332	0.4096	0.9099
H2-C46	0.4174	0.4021	1.0682
H3-C46	0.4013	0.3611	0.8992

Table 8 (Continued) (d) Final thermal parameters (x 10^6)

Atom	β_{11}	β_{22}	β_{33}	β_{12}	β_{13}	β_{23}
Rh	3246(3)	1919(1)	12318(30)	801(1)	1771(3)	-243(0)
CA	3521(4)	2356(2)	10812(26)	1065(1)	1139(2)	267(0)
CB	2744(3)	2616(2)	12741(31)	481(0)	1694(3)	693(1)
CC	4593(5)	2649(2)	13729(33)	1655(1)	3145(5)	1120(1)
CD	2909(3)	2324(2)	10772(26)	694(1)	1365(2)	502(1)
NA	3366(4)	2457(2)	13056(31)	1153(1)	2193(3)	1303(2)
NB	4362(5)	2245(2)	12104(29)	1829(2)	1293(2)	-238(0)
NC	3481(4)	2589(2)	13695(33)	822(1)	1782(3)	482(1)
ND	4124(4)	2582(2)	11737(28)	1492(1)	1221(2)	-631(1)
C1A	2674(3)	2238(2)	11344(27)	758(1)	470(1)	1361(2)
C2A	3391(4)	2444(2)	10325(25)	1298(1)	1862(3)	1444(2)
C3A	4007(4)	2963(2)	12802(31)	974(1)	2305(4)	852(1)
C4A	3316(4)	3077(2)	13476(32)	735(1)	2517(4)	1148(2)
C5A	3411(4)	3377(2)	12083(29)	1409(1)	1752(3)	2088(3)
C6A	4435(5)	2803(2)	12055(29)	1927(2)	2423(4)	2017(3)
C1B	4349(5)	2389(2)	9169(22)	1697(1)	935(1)	195(0)
C2B	4130(4)	2572(2)	8985(22)	1977(2)	1381(2)	740(1)
C3B	4807(5)	2331(2)	11852(28)	1534(1)	1293(2)	457(1)
C4B	6393(7)	2598(2)	12838(31)	2553(2)	2394(4)	482(1)
C5B	5091(5)	2955(2)	10772(26)	2249(2)	1714(3)	932(1)
C6B	4118(4)	2770(2)	106322(25)	1784(2)	1117(2)	952(1)
C1C	3357(4)	2377(2)	11662(28)	937(1)	1810(3)	1325(2)
C2C	2802(3)	2428(2)	12130(29)	1117(1)	1554(2)	1691(2)
C3C	4491(5)	2584(2)	14860(36)	1319(1)	2661(4)	555(1)
C4C	4531(5)	3523(3)	16084(39)	1830(2)	3038(5)	930(1)
C5C	3765(4)	3569(3)	13234(32)	2039(2)	3043(5)	1909(3)
C6C	4320(5)	2674(2)	14156(34)	1521(1)	2782(4)	666(1)
C1D	3950(4)	2477(2)	11089(27)	1632(1)	1292(2)	-172(0)
C2D	3759(4)	2691(2)	9226(22)	1915(2)	1420(2)	733(1)
C3D	4197(4)	2435(2)	11013(26)	1352(1)	1813(3)	176(0)
C4D	4793(5)	3228(2)	11132(27)	1845(2)	1683(3)	-316(0)
C5D	4510(5)	3028(2)	11544(28)	1532(1)	2442(4)	-433(1)
C6D	4058(4)	2915(2)	14684(35)	1669(1)	2749(4)	470(1)
C1	4712(5)	4132(3)	16418(39)	2407(2)	3616(6)	2425(3)
C2	6827(7)	10521(8)	22509(54)	5407(5)	4761(8)	3217(4)
C3	10738(11)	4474(3)	26399(63)	4282(4)	9461(15)	2482(3)
C4	13354(14)	5149(4)	15427(37)	4607(4)	8050(13)	3081(4)
C5	5669(6)	4148(3)	12404(30)	3087(3)	2783(4)	1314(2)
C6	6336(7)	5432(4)	26568(64)	3153(3)	5938(9)	3580(5)
C7	8057(9)	6539(5)	12796(31)	4605(4)	4116(7)	2378(3)
C8	7062(7)	6897(5)	15709(38)	5139(5)	3673(6)	4111(5)
C9	4592(5)	3956(3)	17990(43)	2374(2)	3872(6)	2262(3)
C10	14523(15)	11418(8)	35497(85)	10447(9)	11494(18)	9774(13)
C11	8936(9)	10515(8)	45880(110)	5885(5)	6390(10)	-7435(10)

Table 8 (d) (Continued)

Atom	β_{11}	β_{22}	β_{33}	β_{12}	β_{13}	β_{23}
C12	9397(10)	7288(5)	47456(114)	5415(5)	15552(25)	7580(10)
C13	6086(6)	4535(3)	17487(43)	1874(2)	5534(9)	-129(0)
C14	8168(9)	6553(5)	31789(76)	1122(1)	9525(15)	-292(0)
C15	9906(11)	19041(14)	17904(43)	2467(2)	8110(13)	4473(6)
C16	11454(12)	7675(6)	42929(103)	5477(5)	15830(25)	5219(7)
C17	4557(5)	2201(2)	12176(29)	1341(1)	1960(3)	1521(2)
C18	4857(5)	2063(2)	11984(29)	1199(1)	1629(3)	877(1)
C19	4241(4)	2358(2)	12540(30)	1358(1)	2818(4)	1802(2)
C20	4162(4)	1992(1)	10707(26)	1200(1)	1766(3)	367(0)
O1	5080(5)	2418(2)	13211(32)	1613(1)	3802(6)	1813(2)
O2	3738(4)	2555(2)	11410(27)	1229(1)	1301(2)	131(0)
O3	4213(4)	2775(2)	16307(39)	1714(2)	3921(6)	2166(3)
O4	3906(4)	2889(2)	10155(24)	1539(1)	1399(2)	87(0)
B	5189(6)	2719(2)	8497(20)	1622(1)	1493(2)	799(1)
C21	5257(6)	2553(2)	10228(25)	1395(1)	1966(3)	1410(2)
C22	10520(11)	3241(2)	9444(23)	1073(1)	3061(5)	709(1)
C23	14465(15)	4646(3)	10747(26)	2193(2)	5152(8)	2202(3)
C24	10736(11)	4496(3)	15180(36)	2065(2)	5081(8)	4213(6)
C25	8692(9)	3189(2)	12795(31)	1086(1)	3485(6)	1887(2)
C26	5817(6)	2955(2)	10216(24)	1576(1)	2335(4)	1622(2)
C27	4833(5)	2225(2)	9413(23)	1350(1)	1621(3)	1885(2)
C28	4787(5)	2778(2)	10748(26)	675(1)	1010(2)	1261(2)
C29	5558(6)	3144(2)	12033(29)	1073(1)	741(1)	2130(3)
C30	6007(6)	3296(2)	10756(26)	1251(1)	794(1)	1239(2)
C31	7811(8)	3520(3)	8310(20)	1750(2)	2269(4)	701(1)
C32	6012(6)	3319(2)	11363(27)	2200(2)	2248(4)	2102(3)
C33	5571(6)	2852(2)	8395(20)	1737(2)	1148(2)	873(1)
C34	8128(9)	2702(2)	8916(21)	2300(2)	1157(2)	1278(2)
C35	10613(11)	3531(3)	13605(33)	3051(3)	1197(2)	2359(3)
C36	11061(12)	3737(3)	13156(32)	3972(3)	-1273(2)	612(1)
C37	7546(8)	5227(4)	13803(33)	3877(3)	-777(1)	-2020(3)
C38	5567(6)	3586(3)	12155(29)	1870(2)	845(1)	-527(1)
C39	5653(6)	2518(2)	9027(22)	1332(1)	1010(2)	210(0)
C40	6309(7)	3144(2)	10195(24)	2125(2)	171(0)	-58(0)
C41	6411(7)	4100(3)	15054(36)	2353(2)	290(0)	-666(1)
C42	5241(6)	4485(3)	21330(51)	2362(2)	669(1)	-1400(2)
C43	6130(6)	4642(3)	18168(44)	1835(2)	4295(7)	1486(2)
C44	5617(6)	4068(3)	12982(31)	1765(2)	3033(5)	2306(3)
N1	11394(12)	6141(4)	38190(92)	4056(4)	-328(1)	4444(6)
C45	7471(8)	4286(3)	17431(42)	1217(1)	-478(1)	1849(2)
C46	8104(9)	6124(4)	19498(47)	1665(1)	2737(4)	2634(3)
N2	9373(10)	7322(5)	33699(81)	1204(1)	-143(0)	-2142(3)
C47	12648(13)	8063(6)	31482(75)	1098(1)	-843(1)	369(0)

Table 9. Bond distances (Å)

Rh-CA	1.956(7)	C2D-C30	1.38(1)	B-C21	1.64(1)
Rh-CB	1.976(7)	C3D-C4D	1.39(1)	B-C27	1.67(1)
Rh-CC	1.974(8)	C4D-C5D	1.39(1)	B-C33	1.65(1)
Rh-CD	1.955(7)	C5D-C6D	1.39(1)	B-C39	1.67(1)
CA-NA	1.150(9)	C6D-C1D	1.39(1)	C21-C22	1.38(1)
CB-NB	1.146(9)	C5A-C1	1.53(1)	C22-C23	1.37(1)
CC-NC	1.147(9)	C1-C2	1.52(2)	C23-C24	1.37(2)
CD-ND	1.170(9)	C1-C3	1.54(1)	C24-C25	1.36(1)
NA-C1A	1.406(8)	C1-C4	1.52(1)	C25-C26	1.38(1)
NB-C1B	1.396(9)	C5B-C5	1.53(1)	C26-C21	1.38(1)
NC-C1C	1.386(9)	C5-C6	1.52(1)	C27-C28	1.39(1)
ND-C1D	1.390(9)	C5-C7	1.55(1)	C28-C29	1.40(1)
C1A-C2A	1.39(1)	C5-C8	1.53(1)	C29-C30	1.37(1)
C2A-C3A	1.38(1)	C5C-C9	1.51(1)	C30-C31	1.36(1)
C3A-C4A	1.38(1)	C9-C10	1.50(2)	C31-C32	1.41(1)
C4A-C5A	1.38(1)	C9-C11	1.49(2)	C32-C27	1.41(1)
C5A-C6A	1.39(1)	C9-C12	1.52(2)	C33-C34	1.40(1)
C6A-C1A	1.37(1)	C50-C13	1.52(1)	C34-C35	1.38(1)
C1B-C2B	1.38(1)	C13-C14	1.49(2)	C35-C36	1.37(2)
C2B-C3B	1.39(1)	C13-C15	1.49(2)	C36-C37	1.39(2)
C3B-C4B	1.39(1)	C13-C16	1.54(2)	C37-C38	1.39(1)
C4B-C5B	1.40(1)	C2A-O1	1.369(8)	C38-C33	1.41(1)
C5B-C6B	1.38(1)	O1-C17	1.446(8)	C39-C40	1.42(1)
C6B-C1B	1.38(1)	C17-C18	1.504(11)	C40-C41	1.39(1)
C1C-C2C	1.38(1)	C18-O2	1.437(9)	C41-C42	1.38(2)
C2C-C3C	1.36(1)	O2-C2B	1.352(8)	C42-C43	1.36(2)
C3C-C4C	1.40(1)	C2C-O3	1.368(8)	C43-C44	1.39(1)
C4C-C5C	1.40(1)	O3-C19	1.443(8)	C44-C39	1.39(1)
C5C-C6C	1.39(1)	C19-C20	1.489(10)	C45-C46	1.35(2)
C6C-C1C	1.38(1)	C20-O4	1.435(8)	C45-N1	1.13(2)
C1D-C2D	1.39(1)	O4-C2D	1.366(8)	C47-$\overline{C47}^a$	1.48(4)
				C47-N2	1.41(4)

[a] $\overline{C47}$ is inversion related to C47.

Table 10. Bond angles (°)

CA-Rh-CB	87.5(3)	C5D-C6D-C1D	120.8(7)	C19-C20-C4	107.7(6)
CA-Rh-CC	171.6(3)	C6A-C5A-C1	121.8(7)	C20-O4-C2D	117.3(5)
CA-Rh-CD	90.4(3)	C4A-C5A-C1	121.5(7)	C1D-C2D-O4	116.3(6)
CB-Rh-CC	90.6(3)	C5A-C1-C2	109.3(8)	C3D-C2D-O4	124.9(6)
CB-Rh-CD	172.5(3)	C5A-C1-C3	112.1(8)	C21-B-C27	108.5(6)
CC-Rh-CD	90.4(3)	C5A-C1-C4	108.0(8)	C21-B-C33	110.4(6)
Rh-CA-NA	174.0(6)	C2-C1-C3	109.2(10)	C21-B-C39	110.6(6)
Rh-CB-NB	176.7(6)	C2-C1-C4	110.6(9)	C27-B-C33	105.5(6)
Rh-CC-NC	177.3(7)	C3-C1-C4	107.6(9)	C27-B-C39	110.8(6)
Rh-CD-ND	172.9(6)	C4B-C5B-C5	120.0(7)	C33-B-C39	110.9(6)
CA-NA-C1A	171.9(7)	C6B-C5B-C5	123.4(7)	B-C21-C22	122.4(7)
CB-NB-C1B	176.8(7)	C5B-C5-C6	111.4(7)	B-C21-C26	122.2(7)
CC-NC-C1C	172.3(8)	C5B-C5-C7	109.1(7)	C26-C21-C22	115.3(7)
CD-ND-C1D	172.0(7)	C5B-C5-C8	109.6(7)	C21-C22-C23	123.2(9)
NA-C1A-C2A	118.8(6)	C5B-C5-C7	109.6(8)	C22-C23-C24	120.2(9)
NA-C1A-C6A	118.4(6)	C5B-C5-C8	108.7(8)	C23-C24-C25	118.3(10)
C6A-C1A-C2A	122.2(6)	C7-C5-C8	108.4(8)	C24-C25-C26	121.2(9)
C1A-C2A-C3A	117.8(6)	C4C-C5C-C9	122.3(7)	C25-C26-C21	121.8(8)
C2A-C3A-C4A	119.3(7)	C6C-C5C-C9	121.0(7)	B-C27-C28	121.6(6)
C3A-C4A-C5A	123.5(7)	C5C-C9-C10	108.6(10)	B-C27-C32	122.7(7)
C4A-C5A-C6A	116.6(7)	C5C-C9-C11	112.8(8)	C32-C27-C28	115.6(7)
C5A-C6A-C1A	120.5(7)	C5C-C9-C12	111.2(8)	C27-C28-C29	122.8(7)
NB-C1B-C2B	119.1(6)	C10-C9-C11	105.4(12)	C28-C29-C30	120.3(8)
NB-C1B-C6B	118.3(6)	C10-C9-C12	107.6(11)	C29-C30-C31	118.8(8)
C6B-C1B-C2B	122.5(6)	C11-C9-C12	110.9(12)	C30-C31-C32	121.5(8)
C1B-C2B-C3B	117.2(6)	C4D-C5D-C13	120.5(7)	C31-C32-C27	120.9(8)
C2B-C3B-C4B	120.1(7)	C6D-C5D-C13	122.8(7)	B-C33-C34	123.4(7)
C3B-C4B-C5B	122.6(7)	C5D-C13-C14	113.0(9)	B-C33-C38	122.6(7)
C4B-C5B-C6B	116.5(7)	C5D-C13-C15	108.7(9)	C38-C33-C34	113.4(7)
C5B-C6B-C1B	121.2(7)	C5D-C13-C16	109.5(9)	C33-C34-C35	124.3(8)
NC-C1C-C2C	118.7(6)	C14-C13-C15	110.3(13)	C34-C35-C36	119.7(9)
NC-C1C-C6C	118.7(6)	C14-C13-C16	106.4(10)	C35-C36-C37	119.2(9)
C6C-C1C-C2C	122.3(6)	C15-C13-C16	108.9(14)	C36-C37-C38	119.8(9)
C1C-C2C-C3C	118.0(6)	C1A-C2A-O1	118.4(6)	C37-C38-C33	123.6(8)
C2C-C3C-C4C	120.5(7)	C3A-C2A-O1	123.8(6)	B-C39-C40	122.3(7)
C3C-C4C-C5C	122.0(7)	C2A-O1-C17	115.0(5)	B-C39-C44	122.4(7)
C4C-C5C-C6C	116.7(7)	O1-C17-C18	110.4(6)	C44-C39-C40	115.2(7)
C5C-C6C-C1C	120.5(7)	C17-C18-O2	108.3(6)	C39-C40-C41	121.2(8)
ND-C1D-C2D	117.6(6)	C18-O2-C2B	118.4(5)	C40-C41-C42	121.5(9)
ND-C1D-C6D	120.8(6)	C1B-C2B-O2	117.0(6)	C41-C42-C43	117.8(9)
C6D-C1D-C2D	121.5(7)	C3B-C2B-O2	125.8(6)	C42-C43-C44	121.7(10)
C1D-C2D-C3D	118.8(6)	C1C-C2C-O3	117.2(6)	C43-C44-C39	122.3(7)
C2D-C3D-C4D	119.0(7)	C3C-C2C-O3	124.7(6)	C46-C45-N1	178(1)
C3D-C4D-C5D	123.2(7)	C2C-O3-C19	116.3(5)	C47-C47-N2	172(3)
C4D-C5D-C6D	116.7(7)	O3-C19-C20	107.2(6)		

in such a manner to position one metal atom over another and lead to short interactions between the stacks. In this particular case, indeed, some tendency is found to stack complexes on top of each other. However, the centers of the two $Rh(C\equiv N)_4$ moieties are shifted with respect to one another in the unit cell such that the angle between the rhodium-rhodium vector and the normal to the least-squares plane at the rhodium position is 22.7°, and increases the Rh-Rh distance from the 3.133 Å distance between planes to a value of 3.384(2) Å. This distance is rather long for metal-metal bonding. In $[Rh_2(CNPh)_8](BPh_4)_2$, for example, the relatively weak Rh-Rh bond is 3.19 Å (30). In $[Rh(CO)(PPh_3)_2]_2$ (37) and $Rh_2(DMG)_2(PPh_3)_2\ C_3H_7OH$ (38), the Rh-Rh distances are much shorter than in the title compound; both bonds are under 3.0 Å. Carbon CC lies almost directly below the inversion-related rhodium; their interatomic distance is 3.18 Å. This decreases the possibility of any metal orbital overlap perpendicular to these planes. Electronic interactions of the rhodium atoms with those in other unit cells are negligible as the next shortest Rh-Rh distance is 8.1 Å.

The geometry about the rhodium atom is nearly square planar although there is some pyramidal distortion of the carbons away from the other cation in the cell. This distortion is indicated by a least-squares plane based on the $R-C_4$ group. The carbons, on the average, deviate from this calculated plane by +0.03 Å; the rhodium by -0.11 Å. The average Rh-C bond length is 1.965 Å. This agrees well with the 1.96 Å distance reported for $[RhI(fumaronitrile)P(OC_6H_5)_3(p\text{-}CH_3OC_6H_4NC_2)]$ (39) and the 1.94 Å length for $[Rh(CNPh_4)(BPh_4)_2]$ (30). In both of these

Table 11. Equations of least squares planes and interplanar angles

Atom	Distance from Plane (Å)	Atom	Distance from Plane (Å)
	Plane I fitting Rh, CA, CB, CC, CD		
	-0.02958 X + 0.52967 Y - 0.84768 Z - 1.50335 = 0		
Rh	-0.1068	CC	0.0348
CA	0.0345	CD	0.0192
CB	0.0182		
	Plane II fitting C1A, C2A, C3A, C4A, C5A, C6A		
	0.4461 X - 0.44312 Y + 0.77843 Z - 1.76900 = 0		
NA	-0.1091	C5A	0.0090
C1A	0.0150	C6A	-0.0190
C2A	-0.0009	O1	-0.0748
C3A	-0.0092	C17	-0.9947
C4A	0.0050		
	Plane III fitting C1B, C2B, C3B, C4B, C5B, C6B		
	0.20049 X - 0.42583 Y + 0.88230 Z - 0.11359 = 0		
NB	0.0669	C5B	-0.0088
C1B	-0.0006	C6B	0.0091
C2B	-0.0080	O2	-0.0325
C3B	0.0082	C18	0.2745
C4B	0.0001		
	Plane IV fitting C1C, C2C, C3C, C4C, C5C, C6C		
	-0.11609 X + 0.46452 Y - 0.87791 Z - 1.04124 = 0		
NC	-0.1242	C5C	0.0127
C1C	-0.0011	C6C	-0.0094
C2C	0.0084	O3	0.0979
C3C	-0.0048	C19	-0.7950
C4C	-0.0057		
	Plane V fitting C1D, C2D, C3D, C4D, C5D, C6D		
	0.51987 X - 0.51866 Y + 0.67875 Z - 0.95001 = 0		
ND	-0.0850	C5D	-0.0058
C1D	-0.0017	C6D	0.0059
C2D	-0.0025	O4	-0.3880
C3D	0.0024	C20	-1.4365
C4D	0.0017		

Table 11 (Continued)

Interplanar Angles		
Plane	Plane	Angle (°)
I	II	155.19
I	III	168.35
I	IV	6.44
I	V	149.93
II	III	15.27
II	IV	160.19
II	V	8.37
III	IV	174.67
III	V	22.48
IV	V	153.79

compounds, the average C-N-C bond angle is 176°. The average metal-C-N angle is 176° in the former and 174° in the latter. These are comparable to the equivalent angles (173° for C-N-C bonds and 175° for C-N-C bonds) observed in this compound.

The bond distances and angles in the ligands are unexceptional. The average phenyl C-C bond length is 1.386 Å; the average ring angle is 119°. These agree well with the values in benzene, 1.393(5) Å and 120° (14). Least-squares planes fitting the ring atoms are given in Table 11. These planes indicate only slight deviations from planarity. The interplanar angle between phenyl rings A and B is 15.27°, whereas the angle between rings C and D is 26.21°. This difference can be attributed to steric effects. Ring D approaches the tetraphenylborate anion quite closely. The shortest contacts are 3.54 Å between C3D and C34 and 3.01 Å between their hydrogens. If this plane were tilted the same with respect to ring C as rings A and B are to each other, these distances would be shortened even further. The closest solvent-cation contact is 3.35 Å between O3 and C46. This also may contribute to the large angle between the C and D ring planes.

The oxygen-phenyl carbon distances average 1.364 Å. This agrees well with the 1.366 Å bond length reported for bis-4-methoxyphenyl nitroxide (40). The other type of oxygen-carbon bond averages 1.440 Å in length, which is comparable to 1.43 Å in diethyl ether (14).

There are no unusual features in the anion. The three solvent molecules exhibit large thermal motion, an artifact which is due to their apparent disorder.

The large anion affects the molecular packing. Examination of the structures of this cation with other less bulky counterions and the variations in molecular packing could prove quite interesting as other stacking arrangements including the cation could result.

THE CRYSTAL AND MOLECULAR STRUCTURE OF BIS(CIS-2-METHOXY-4,6-DIMETHYL-1,3,2-DIOXAPHOSPHORINANE)TETRACARBONYL-MOLYBDENUM(0), A COMPLEX CONTAINING A THERMODYNAMICALLY UNSTABLE LIGAND ISOMER

Introduction

The phosphorinane ligand exists in two forms -- one with the phosphorus lone pair axial and the other with the lone pair equitorial. The axial lone pair form is reported to be the less stable form thermodynamically (41). As has been shown in Dr. Verkade's group, both these ligands readily coordinate to transition metals. Spectroscopic investigations have shown that it is possible to obtain two forms of cis-$(ligand)_2Mo(CO)_4$ complex. From mass spectrophotometry and from the number and relative intensities of the peaks on the infrared spectra, it was inferred that both compounds had cis geometries. However, differences in melting points (99-100° for the title compound compared to 76° for the other form), C-CH_3 NMR shifts (1.33δ for the former, 1.28δ for the latter), and CO frequencies (2038, 1942, 1914 cm^{-1} for the former, 2040, 1945, 1924 cm^{-1} for the latter) suggested the phosphorus ligands coordinated with the retention of the phosphorus configuration (42). In order to verify (or disprove) these inferences, a complete molecular structure investigation of the title compound was carried out utilizing single crystal X-ray diffraction techniques.

Experimental

Crystal Data $MoP_2O_{10}C_{16}H_{22}$, M.W. = 532.3, monoclinic, $P2_1/c$, $\underline{a}$ = 12.220(3), $\underline{b}$ = 9.963(2), $\underline{c}$ = 20.150(6) Å, β = 103.01(3)°, V = 2390.1 $Å^3$, ρ_{calc} = 1.48 g/cm^3, μ = 7.21 cm^{-1} (Mo K_α, λ = 0.70954 Å).

A sample of the title compound was obtained from R. A. Montag and Dr. J. G. Verkade. The crystals were grown by slow evaporation from a pentane solution in a nitrogen atmosphere. A crystal was sealed in a Lindeman capillary under nitrogen and mounted on the fully-automated four-circle Ames Laboratory diffractometer.

Eleven reflections from initial ω-oscillation photographs were used to index the cell (2). The cell scalars indicated monoclinic symmetry, which was then verified by the presence of a mirror on the $\underline{b}$-axial photograph. Four octants of data were collected at room temperature with graphite-monochromated Mo K_α radiation. Within a 2θ sphere of 50°, 4890 intensities were measured. Repeated measurements of three standard reflections during the course of data collection indicated the crystal as well as the electronics were quite stable.

Corrections for the Lorentz and polarization effects were made; no absorption correction was deemed necessary. Equivalent, observed ($Fo \geq 3\sigma Fo$) reflections were averaged leaving 2057 data. During the course of refinement, it was noted that the magnitude of high angle reflections were all very small; consequently, all F values with $2\theta > 42.3^\circ$ were discarded. Large thermal motion effects were suspected to contribute to this. Upon refinement, these thermal motion effects were confirmed to be large. In the final least-squares cycles, 1588 reflections were used.

The ±2θ of eleven strong independent reflections were used to obtain refined lattice parameters.

An analysis of the data revealed two systematic absences: hOℓ ℓ = 2n+1 and OkO, k = 2n+1, indicating space group $P2_1/c$. A Howells, Phillips, and Rogers test (34) indicated a center of symmetry supporting this choice.

The position of the metal atom was determined from the examination of a Patterson function. Successive least-squares refinements (35) and electron density map calculations (36) were used to locate the remaining non-hydrogen atoms. Full-matrix anisotropic refinement gave an R, the conventional residual index, of 10.7% and a weighted R of 13.3%. The large thermal disorder prevented further refinement. Although data collected at a reduced temperature could lessen the thermal motion, the important structural features were clearly determined by the room temperature data, and therefore, an additional low temperature study did not seem warranted.

ORTEP (10) drawings of this molybdenum complex and its unit cell are shown in Figures 9 and 10. Atomic parameters and intramolecular bond distances and angles are given in Tables 12 and 13, respectively.

Discussion

In Figure 9, it can be seen that the molybdenum atom occupies the axial position of the six-membered ring of each of the phosphorus ligands, thus confirming that the coordination process occurs with retention of the phosphorus configuration. The $P(OC)_2$ moiety can be

Figure 9. A computer-generated drawing of $MoP_2O_{10}C_{16}H_{22}$, excluding the hydrogen atoms

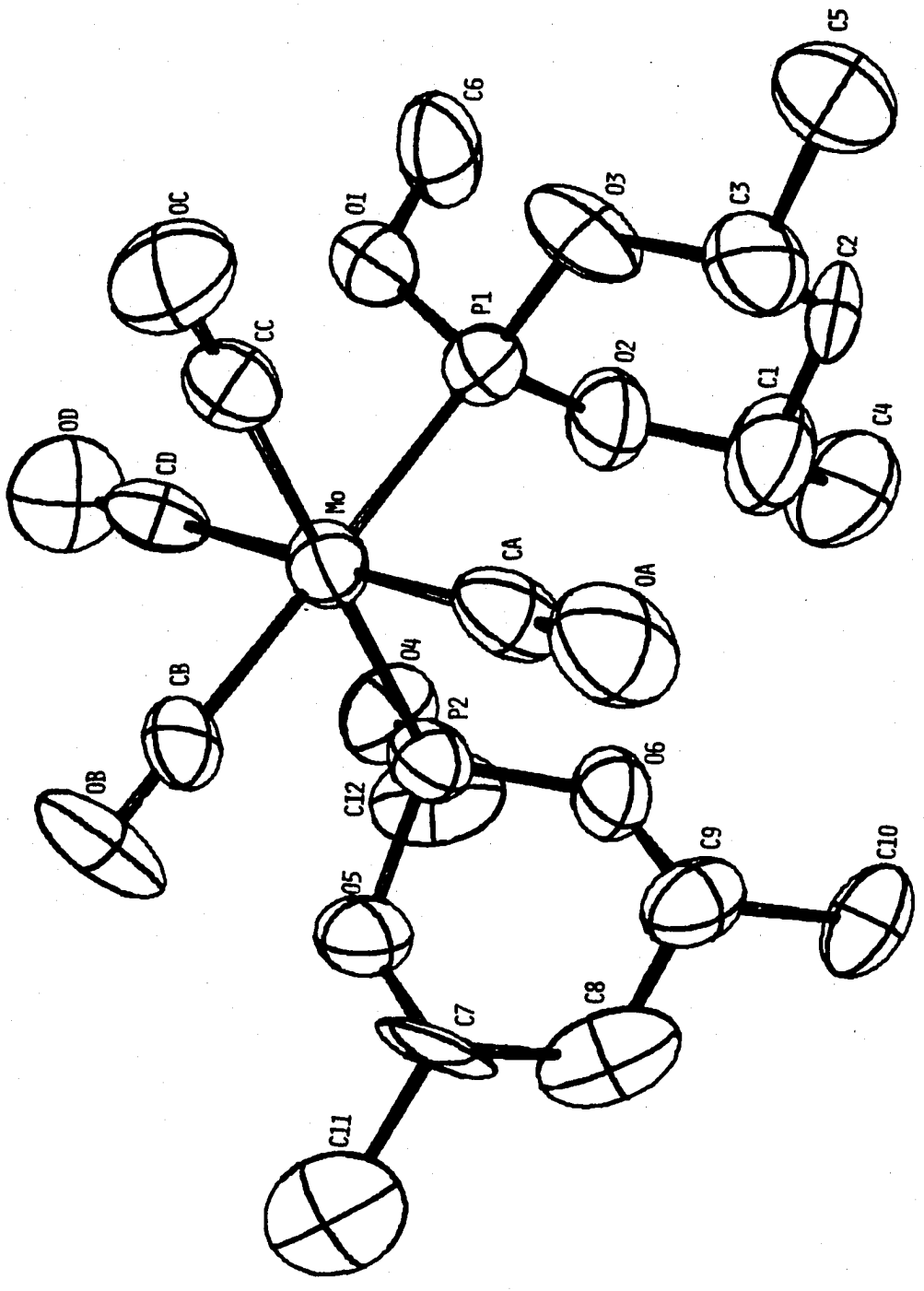
C5
C6
O1
O3
C3
OC
C2
P1
CC
O2
C1
C4
OD
CD
Mo
CA
OA
O4
CB
P2
O6
C12
OB
C9
C10
O5
C8
C7
C11

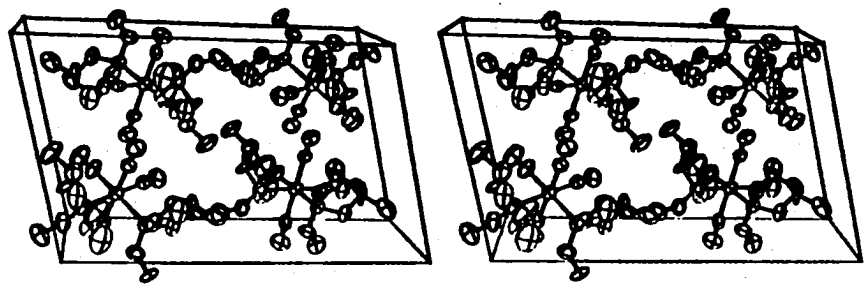

Figure 10. Unit cell stereograph of $MoP_2O_{10}C_{16}H_{22}$

Table 12. Final atomic positional and thermal parameters for $MoP_2O_{10}C_{16}H_{22}$

(a) Positional parameters

Atom	x	y	z
Mo	0.2789(2)	0.1636(2)	0.1813(1)
P1	0.2450(6)	-0.0015(7)	0.0882(3)
P2	0.1657(6)	0.0274(6)	0.2433(3)
OA	0.5051(20)	0.0361(24)	0.2594(11)
OB	0.3147(16)	0.3780(21)	0.2986(10)
OC	0.4149(19)	0.3402(22)	0.0979(12)
OD	0.0540(18)	0.3069(23)	0.1029(11)
CA	0.4212(24)	0.0767(31)	0.2307(14)
CB	0.3054(20)	0.3038(24)	0.2585(14)
CC	0.3679(24)	0.2758(27)	0.1285(14)
CD	0.1333(26)	0.2537(27)	0.1298(13)
C1	0.4248(25)	-0.1534(43)	0.0889(14)
C2	0.3453(31)	-0.2736(30)	0.0874(17)
C3	0.2693(35)	-0.2517(32)	0.1315(18)
C4	0.5106(26)	-0.1788(39)	0.0435(18)
C5	0.1842(40)	-0.3749(34)	0.1275(20)
C6	0.1259(25)	-0.0288(31)	-0.0385(14)
C7	0.2367(32)	0.0678(34)	0.3752(15)
C8	0.2450(27)	-0.0828(32)	0.3839(14)
C9	0.2916(22)	-0.1421(27)	0.3269(14)
C10	0.2937(31)	-0.3034(29)	0.3382(15)
C11	0.1814(29)	0.1393(35)	0.4357(16)
C12	-0.0411(24)	-0.0760(32)	0.2254(15)
O1	0.1638(15)	0.0567(18)	0.0246(8)
O2	0.3450(14)	-0.0463(20)	0.0567(9)
O3	0.1892(16)	-0.1447(16)	0.0979(9)
O4	0.0416(12)	0.0055(18)	0.2006(8)
O5	0.1461(15)	0.0869(17)	0.3146(8)
O6	0.2052(15)	-0.1196(16)	0.2661(9)

Table 12 (Continued) (b) Thermal parameters

Atom	β(1,1)	β(2,2)	β(3,3)	β(1,2)	β(1,3)	β(2,3)
Mo	0.0073(2)	0.0090(3)	0.0031(1)	0.0002(2)	0.0017(1)	0.0000(1)
P1	0.0089(7)	0.0106(8)	0.0030(2)	0.0014(6)	0.0020(3)	0.0009(3)
P2	0.0080(6)	0.0111(9)	0.0031(2)	0.0002(6)	0.0020(3)	-0.0004(4)
OA	0.010(2)	0.023(4)	0.005(1)	0.003(3)	0.002(1)	-0.001(1)
OB	0.013(2)	0.021(3)	0.004(1)	0.001(2)	0.002(1)	-0.006(1)
OC	0.018(2)	0.019(3)	0.006(1)	0.000(2)	0.006(1)	0.003(2)
OD	0.010(2)	0.022(4)	0.005(1)	0.000(2)	0.000(1)	0.000(1)
CA	0.006(3)	0.019(4)	0.003(1)	0.002(3)	0.001(1)	-0.002(2)
CB	0.006(2)	0.010(3)	0.003(1)	0.003(2)	0.001(1)	0.000(1)
CC	0.011(2)	0.015(3)	0.004(1)	0.004(3)	0.004(1)	0.001(2)
CD	0.009(3)	0.016(4)	0.002(1)	-0.001(3)	0.001(1)	-0.002(1)
C1	0.011(3)	0.024(7)	0.004(1)	0.008(4)	0.002(1)	0.001(2)
C2	0.022(4)	0.011(4)	0.004(1)	0.011(3)	0.003(2)	0.003(2)
C3	0.018(5)	0.017(5)	0.008(2)	0.006(4)	0.007(2)	0.006(2)
C4	0.014(3)	0.028(7)	0.007(2)	0.007(4)	0.007(2)	0.003(3)
C5	0.029(7)	0.015(5)	0.007(2)	-0.002(5)	0.006(3)	0.003(2)
C6	0.014(3)	0.016(5)	0.004(1)	0.006(3)	-0.001(1)	-0.001(2)
C7	0.025(5)	0.015(5)	0.002(1)	-0.002(4)	0.004(2)	-0.004(2)
C8	0.009(3)	0.024(5)	0.003(1)	-0.008(3)	-0.001(1)	0.001(2)
C9	0.007(2)	0.019(4)	0.003(1)	0.002(3)	0.001(1)	0.002(2)
C10	0.021(4)	0.011(4)	0.005(1)	0.002(3)	0.003(2)	0.004(2)
C11	0.014(4)	0.021(5)	0.005(1)	-0.011(4)	-0.001(1)	-0.001(2)
C12	0.011(3)	0.025(5)	0.005(1)	-0.011(3)	0.004(1)	0.001(2)
O1	0.013(2)	0.015(3)	0.003(1)	0.004(2)	0.002(1)	0.000(1)
O2	0.006(2)	0.020(3)	0.005(1)	0.000(2)	0.004(1)	-0.002(1)
O3	0.013(2)	0.010(2)	0.005(1)	0.001(2)	0.003(1)	0.001(1)
O4	0.007(1)	0.018(2)	0.004(1)	0.001(2)	0.000(1)	0.001(1)
O5	0.013(2)	0.013(2)	0.003(1)	-0.001(1)	0.003(1)	0.000(1)
O6	0.011(2)	0.009(2)	0.004(1)	0.001(2)	0.003(1)	0.001(1)

Table 13. Intramolecular bond distances and angles

		Distances (Å)			
P1-Mo	2.459(7)	O5-P2	1.62(2)	CD-OD	1.13(4)
P2-Mo	2.468(7)	O6-P2	1.58(2)	C2-C1	1.54(5)
CA-Mo	2.00(3)	C12-O4	1.47(3)	C4-C1	1.56(5)
CB-Mo	2.06(3)	C1-O2	1.46(4)	C3-C2	1.44(5)
CC-Mo	2.02(3)	C7-O5	1.46(4)	C9-C10	1.57(4)
CD-Mo	2.05(3)	C3-O3	1.50(4)	C5-C3	1.60(5)
O1-P1	1.55(2)	C9-O6	1.45(3)	C7-C11	1.68(5)
O2-P1	1.62(2)	CA-OA	1.13(3)	C7-C8	1.51(5)
O3-P1	1.61(2)	CB-OB	1.08(3)	C8-C9	1.53(4)
O4-P2	1.58(2)	CC-OC	1.13(4)	O1-C6	1.51(3)
		Angles (°)			
P1-Mo-P2	90.0(2)			O4-P2-O6	102.9(10)
P1-Mo-CA	93.9(8)			O5-P2-O6	100.2(9)
P1-Mo-CB	179.1(7)			P2-O4-C12	122.7(16)
P1-Mo-CC	89.2(8)			P1-O1-C6	120.2(16)
P1-Mo-CD	85.9(8)			P1-O2-C1	120.0(17)
P2-Mo-CA	92.0(8)			P1-O3-C3	115.4(18)
P2-Mo-CB	90.1(7)			P2-O5-C7	117.1(17)
P2-Mo-CC	178.4(8)			P2-O6-C9	122.6(16)
P2-Mo-CD	88.6(8)			Mo-CA-OA	175.1(25)
CA-Mo-CB	87.0(10)			Mo-CB-OB	177.2(21)
CA-Mo-CC	89.5(10)			Mo-CC-OC	178.0(26)
CA-Mo-CD	179.4(11)			Mo-CE-OD	177.6(25)
CB-Mo-CC	90.7(11)			O2-C1-C2	103.4(24)
CB-Mo-CD	93.2(10)			O2-C1-C4	107.2(25)
CC-Mo-CD	89.6(11)			O3-C3-C2	106.0(28)
Mo-P1-O1	110.3(7)			O5-C7-C8	104.2(23)
Mo-P1-O2	118.1(7)			O5-C7-C11	101.2(25)
Mo-P1-O3	120.2(7)			O6-C9-C8	103.4(20)
Mo-P2-O4	112.3(7)			O6-C9-C10	107.1(21)
Mo-P2-O5	117.3(7)			C1-C2-C3	110.9(27)
Mo-P2-O6	119.2(7)			C2-C1-C4	111.6(29)
O1-P1-O2	101.3(10)			C8-C7-C11	111.7(24)
O1-P1-O3	102.8(10)			C5-C3-C2	110.4(29)
O2-P1-O3	101.4(10)			C8-C9-C10	107.8(23)
O4-P2-O5	102.6(10)			C9-C8-C7	110.9(24)

best described as a somewhat flattened chair form of the ring. The average POC ring angle is 118.8° and the average OPO ring angle is 100.8°. This flattening helps avoid severe 1,3 interactions of axial hydrogens and the $Mo(CO)_4$ moiety.

These POC and OPO ring angles agree well with those observed in complexes containing $P(OCH_3)_3$ ligands. In trans-$Fe(CO)_3(P(OCH_3)_3)_2$, for example, these angles average 121.0° and 100.9°, respectively (43). The crystal structure of cis-$Mo(CO)_4[P(OCH_3)_3]NHC_5H_{10}$ also contains 100.1° O-P-O angles (44). The Mo-P-O bond angles average 120.6° in this latter example. The equivalent value in the title compound is 116°. The mean values of the Mo-P, P-O, and O-C bond lengths are 2.464 Å, 1.59 Å, and 1.46 Å, respectively. The Mo-P and P-O distances in cis-$Mo(CO)_4[P(OCH_3)_3]NHC_5H_{10}$ are 2.462 Å and 1.57 Å, respectively. In the iron complex, the P-O bonds average 1.59 Å and the O-C bonds average 1.44 Å.

There are no unusual distances in the molybdenum-carbonyl portion of the structure. The average Mo-C (2.03 Å) and C-O (1.12 Å) values are consistent with those observed in hexacarbonylmolybdenum(0) (2.08(4) Å and 1.15(5) Å, respectively) (14).

There are no short intermolecular contacts. The shortest such distance is 3.95 Å between C4 generated by the c-glide (x, 1/2-y, 1/2+z) and C4 generated by the two-fold screw (1-x, 1/2+y, 1/2-z).

AN ALGORITHM FOR EMPIRICAL ABSORPTION CORRECTION

Introduction

The intensity of an X-ray beam is diminished as it passes through a crystal due to absorption. This intensity, I, after passing through a length t of absorber is given by the equation $I = I_o e^{-\mu t}$, where I_o is the incident beam intensity and μ is the linear absorption coefficient.

Reflections have different path lengths through a crystal and so suffer unequal effects due to absorption. When these variations are minor, temperature factors can shift to compensate for them. Often, however, these effects are great enough that one has to correct for them. To do this, one usually has to calculate the path length of each reflection based on a good analytical description of the crystal. This can consume large amounts of computer time and requires a well-formed crystal, so that accurate size and shape measurements can be made. It also ignores the absorption due to mother liquors and mounting materials, such as glass capillaries and glue.

Because of these difficulties with analytical absorption corrections, a means of empirical absorption correction was devised (45,46). This method uses the variation of intensity of a strong reflection near $\chi = \pm 90°$ as the ϕ angle varies to estimate the effects of absorption. A computer program based on this method has been written. To help alleviate any inaccuracies caused by assuming the absorption effects to be solely ϕ-dependent, multiple ϕ-scans with different θ values may be included in the program.

The listing and description of this empirical absorption correction program are given in this section. Its results for various values of μ are also compared with those of TALABS (47,48), an analytical correction program.

Description of the Method

An empirical absorption curve is obtained from the variation in intensities of a strong reflection as the crystal is rotated around a reciprocal lattice vector. Reflections with $\chi = \pm 90°$ are in the reflecting position for all values of ϕ. The variation in intensity of one of these reflections as the crystal is stepped through all values of ϕ in 10° intervals gives a measure of the relative absorption of the X-rays as they pass through the crystal in a direction essentially perpendicular to the rotation axis. A ϕ-scan for $LiZn_2Mo_3O_8$ is given in Figure 11.

The relative intensities $(\frac{I}{I_{max}})$ can be placed on an absolute scale by forcing their average to be equal to $e^{-\mu t_{av}}$, where t_{av} is the average size of the crystal. At any value, $\frac{I}{I_{max}}$ can be set equal to $e^{-\mu 2t/\cos\theta}$, where t is the distance from the center of the crystal to the face in reflecting position and θ is the theta angle at which the ϕ-scan was measured. This distance, t, is equal to $-\log(\frac{I}{I_{max}})\cos\theta/2\mu$. The transmittance for any ϕ-value, $T(\phi)$, is $(\frac{I}{I_{max}})^{\cos\theta}$.

The transmittance for a general hkl reflection, T_{hkl}, is equal to $e^{-\mu(t_{inc} + t_{ref})}$, where t_{inc} and t_{ref} are the path lengths of the incident and reflections beams, respectively. The values of ϕ appropriate to satisfy the restriction that the incident and reflected

Figure 11. ϕ-scan data for $LiZn_2Mo_3O_8$

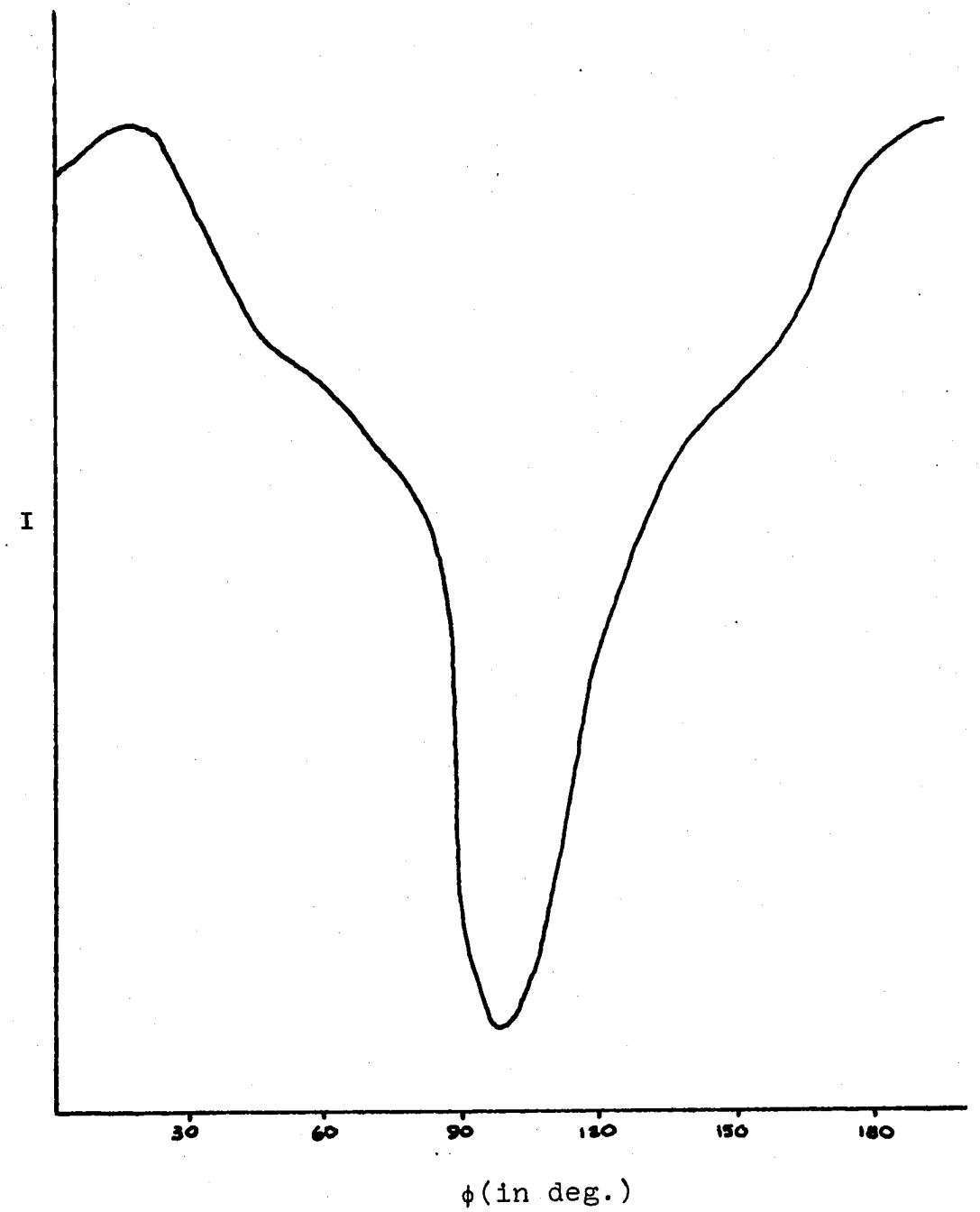
I
30
60
90
120
150
180
ϕ(in deg.)

beams lie in the horizontal plane are ϕ_{inc} and ϕ_{ref}. On a four-circle diffractometer, these are $\phi_{hkl} \mp \tan^{-1}(\tan\theta\cos\chi)$. From ϕ_{inc} and ϕ_{ref}, one can calculate t_{inc} and t_{ref}.

$$t_{inc} = -[\log(\frac{I\phi_{inc}}{I_{max}})]\cos\theta/2\mu \text{ and } t_{ref} = -[\log(\frac{I\phi_{ref}}{I_{max}})]\cos\theta/2\mu.$$

Substituting these values into the equation $T_{hkl} = e^{-\mu(t_{inc} + t_{ref})} = e^{-\mu t_{inc}} \times e^{\mu t_{ref}}$, one obtains T_{hkl}

$$= e^{-\mu\left(-\log(\frac{I\phi_{inc}}{I_{max}})\frac{\cos\theta}{2\mu}\right)} \quad e^{-\mu\left(-\log(\frac{I\phi_{ref}}{I_{max}})\frac{\cos\theta}{2\mu}\right)}.$$

Substituting $T(\phi_{inc})$ and $T(\phi_{ref})$ into this expression gives $T_{hkl} = T(\phi_{inc})^{1/2} \times T(\phi_{ref})^{1/2}$, or the geometric mean of the two transmittances.

This approach is similar to that of North and co-workers (45) except that they use the arithmetic mean, $T_{hkl} = (T(\phi_{inc}) + T(\phi_{ref}))/2$. As noted in the mathematical development described above, the geometric mean seems more appropriate.

A multiple phi scan option was also added in this method. Phi scans are measured at several different theta values; one then has $T(\phi,\theta)$. When calculating T_{hkl}, one uses a linear interpolation of T and θ, thus introducing some θ dependence.

A listing of the program is given in Table 14.

Table 14. The listing of the empirical absorption correction program

```
      PROGRAM ABSN(OUTPUT,INPUT,TAPE5=INPUT,TAPE10,TAPE6=OUTPUT,TAPE20)
C CAVEAT EMPTOR
      DIMENSION PHI(37),F2(8,360),Q(37),THETA(8),COST(8)
      DO 10 I=1,37
      PHI(I)=(I-1)*10.0
   10 CONTINUE
      READ(5,20) NPS,ABSC,TAV
   20 FORMAT(I12,2F10.2)
      SCALE=EXP(-ABSC*TAV)
      DO 90 K=1,NPS
      FMAX=0.0
      READ(5,30) THETA(K)
   30 FORMAT(F10.2)
      COST(K)=COS(0.017456*THETA(K))
      READ(5,40) (F2(K,I),I=1,36)
   40 FORMAT(9F7.2)
      DO 50 I=1,18
      F2(K,I)=(F2(K,I)+F2(K,I+18))/2.0
      F2(K,I+18)=F2(K,I)
      IF(F2(K,I).GT.FMAX) FMAX=F2(K,I)
   50 CONTINUE
      DO 60 J=1,36
      Q(J)=F2(K,J)/FMAX
   60 CONTINUE
      Q(37)=Q(1)
      N=1
      SUM=0.0
      DO 70 I=1,360
      VAR=I-1.0
      IF(VAR.GT.PHI(N+1)) N=N+1
      F2(K,I)=Q(N)+((Q(N+1)-Q(N))*(VAR-PHI(N)))/10.0
      SUM=SUM+F2(K,I)
   70 CONTINUE
      SCALEM=SCALE*360.0/SUM
      DO 80 I=1,360
      F2(K,I)=(F2(K,I)*SCALEM)**COST(K)
   80 CONTINUE
   90 CONTINUE
  100 READ(10,120)NRFL,IH,KI,L,IOM,ICH,IPH,IBK,NSTP,IBT
      IF(EOF(10))210,110
  110 CONTINUE
  120 FORMAT(I5,3I3,3I6,4I8)
      T=0.017453*IOM*0.01
      C=0.017453*ICH*0.01
      V=COS(C)*TAN(T)
      DEL=ATAN(V)*57.29578
```

Table 14 (Continued)

```
      IP=IPH*0.01-DEL+1.5
      IM=IPH*0.01+DEL+1.5
      IF(IM.GT.361) IM=IM-360
      IF(IP.GT.361) IP=IP-360
      IF(IM.LT.1) IM=IM+360
      IF(IP.LT.1) IP=IP+360
      IF(NPS.EQ.1) GO TO 160
      OMEGA=IOM*0.01
      IF(OMEGA.LT.THETA(1)) GO TO 160
      IF(OMEGA.GT.THETA(NPS)) GO TO 150
      DO 130 K=2,NPS
      IF(OMEGA.GT.THETA(K)) GO TO 130
      INT=K
      GO TO 140
  130 CONTINUE
  140 K=INT-1
      T1=SQRT(F2(K,IP)*F2(K,IM))
      T2=SQRT(F2(INT,IP)*F2(INT,IM))
      TGEO=(T2-T1)/(THETA(INT)-THETA(K))*(OMEGA-THETA(K))+T1
      GO TO 180
  150 K=NPS
      GO TO 170
  160 K=1
  170 TGEO=SQRT(F2(K,IP)*F2(K,IM))
  180 PATH=-ALOG(TGEO)/ABSC
      WRITE(20,190) NRFL,IH,KI,L,IOM,ICH,IPH,IBK,NSTP,IBT,TGEO,PATH
  190 FORMAT(I5,3I3,3I6,4I8,2F8.6)
      WRITE(6,200) IH,KI,L,TGEO,PATH
  200 FORMAT(1X,3I5,2F10.6)
      GO TO 100
  210 CONTINUE
      STOP
      END
```

Description of Input Parameters and Required Data Files

The following cards or card images are necessary to run this absorption program:

Card Type	Description
1. Control card	Format(I12,2F10.2)
Columns	
1-12	NPS, the number of ϕ-scans to be input
13-22	ABSC, the absorption coefficient in cm^{-1}
23-33	TAV, the average size of the crystal in cm. This value is not needed if absolute scaling is unnecessary. In practice, the mean of the depth and width of the crystal works well for absolute scaling with $\mu<200$ cm^{-1}. For $\mu\geq200$ cm^{-1}, a slightly underestimated size works better.
2. Theta value of the ϕ-scan	Format(F10.2)
Columns 1-10	THETA(K), the theta value, in degrees, at which the ϕ-scan was measured
3.-6. Phi scan intensity data	Format(9F7.2)

The intensity data, starting at $\phi=0°$ and increasing in 10° increments, is input on four cards.

Card 3 ϕ = 0 to 80°

Card 4 ϕ = 90 to 170°

Card 5 ϕ = 180 to 260°

Card 6 ϕ = 260 to 350°

For multiple ϕ-scans, cards 2-6 are repeated. The phi scans must be arranged in increasing order of the theta value at which they were measured.

The following data files are required:

FILE 5. The standard file number for the card reader.

FILE 6. The standard file number for the line printer.

FILE 10. This contains the raw data. Each record contains NRFL, IH, K, L, ITHETA, ICHI, IPHI, IBK, ITC, NSTP, and IBT. The format is (I5, 3I3, 3I6, 4I8). The angles ITHETA, ICHI, and IPHI are multiplied by 100. IBK and ITC are the background and total counts, respectively. NSTP is the number of steps + 10000 x the number of scans; IBT is a counting time factor.

FILE 20. This is the output file containing the raw data plus the calculated transmission factor, TGEO, and the absorption weighted path-length, PATH. The format is (I5, 3I3, 3I6, 4I8, 2F8.6). This file is to be used as input into a data reduction program.

Comparison of this Program with TALABS

To compare this empirical absorption program with TALABS, an analytical absorption program, a set of angle data with $2\theta \leq 50°$ was generated for a perfectly shaped 0.15 x 0.05 x 0.45 mm rectangular prismatic crystal. Orthorhombic symmetry was assumed with $\underline{a} = 9$, $\underline{b} = 7.5$, and $\underline{c} = 4$ Å, The crystal was then "mounted" so that the orientation matrix, B, $= \begin{bmatrix} a^* & 0 & 0 \\ 0 & b^* & 0 \\ 0 & 0 & c^* \end{bmatrix}$. Its longest dimension was parallel to the ϕ-axis. The complete description of the crystal's orientation is given in Table 15. With this orientation, any 00ℓ reflection has $\chi = 90°$ and is thus suitable for a ϕ-scan.

Table 15. Test crystal orientation

χ (in °)[a]	ϕ (in °)	D[b] (in cm)
0.0	90.0	0.0025
0.0	-90.0	0.0025
0.0	0.0	0.0075
0.0	180.0	0.0075
90.0	0.0	0.0225
-90.0	0.0	0.0225

[a]The angles are those for when the face is in a reflecting position. A face is in a reflecting orientation when it faces the $2\theta = 90°$ position.

[b]The distance from the center of the crystal to the face.

Phi scans were then generated with TALABS by calculating the transmittance of all 00ℓ reflections at 10° intervals in ϕ. These were then used as input for the empirical absorption program. TALABS was run twice. The first run used the exact crystal dimensions; the second run was based upon 10% larger crystal dimensions. The 10% error in size is an estimate of the measuring errors one would introduce in practice. For μ = 124 cm^{-1} and utilizing a single ϕ-scan, the results of TALABS and this program are quite comparable. Table 16 (a) contains the calculated transmittances for selected reflections. The empirical absorption correction almost always is closer to the true transmittance, i.e. the TALABS value with exact crystal dimensions, than TALABS with inexact measurements.

For larger μ's in the range of 200-300 cm^{-1}, using the multiple ϕ-scan option improves the results. A comparison of calculated transmittances for μ = 224 cm^{-1} is given in Table 16 (b). It should be noted, however, that the single ϕ-scan is usually no worse than TALABS with a 10% measurement error. For most reflections, it is quite better.

For extremely large μ's (>400 cm^{-1}), analytical corrections are better than the ϕ-scan program (Table 16 (c)). Absorption coefficients in this range are rarely encountered in organometallics or organic compounds, however.

The cost of the program is significantly less than TALABS. Using the CDC7600 computer at Lawrence Berkeley Lab, this program costs about 0.19¢/reflection. The cost of TALABS varies greatly with the shape of the crystal. A simple crystal completely described by six faces averages

Table 16. Comparisons between TALABS and the empirical absorption correction program

a. $\mu = 124\ cm^{-1}$

H	K	L	Angles (x 10^2) θ	χ	φ	Transmittances (x 10^6) TALABS	Phi Scan	TALABS (10% Measuring Error)
0	0	1	509	9000	9000	160181	164660	134029
0	0	2	1022	9000	9000	162500	164660	136816
0	0	3	1544	9000	9000	162670	164660	137666
0	0	4	2079	9000	9000	160683	164660	136599
0	1	0	271	0	9000	182382	188628	155685
0	1	1	577	6193	9000	186678	188628	160239
0	1	2	1058	7507	9000	188955	188628	162952
0	1	3	1569	7992	9000	189285	188628	163909
0	1	4	2098	8241	9000	187615	188628	163081
0	2	0	543	0	9000	206648	204579	181715
0	2	1	745	4315	9000	212689	204579	186001
0	2	2	1160	6193	9000	214942	212547	188660
0	2	3	1641	7043	9000	215409	212547	189703
0	2	4	2155	7507	9000	214101	212547	189162
0	3	0	816	0	9000	234574	228469	207428
0	3	1	964	3200	9000	238458	228469	211546
0	3	2	1314	5134	9000	240666	228469	214129
0	3	3	1756	6193	9000	241249	228469	215238
0	3	4	2248	6820	9000	240294	236421	214976
0	4	0	1091	0	9000	260360	251775	233010
1	4	0	1115	0	7823	251777	241831	222832
1	4	1	1220	2465	7823	255280	241831	226586
1	4	2	1522	4254	7823	256071	236165	227755
1	4	3	1921	5401	7823	254266	236165	226463
1	4	4	2384	6142	7823	251745	238530	224617
1	5	0	1388	0	8054	279234	258059	250787
1	5	1	1482	2030	8054	282693	258059	254468
1	5	2	1736	3849	8054	284880	265876	256987
1	5	3	2100	4797	8054	285885	265876	258439
1	6	0	1666	0	8209	308468	288628	280146
1	6	1	1746	1720	8209	311623	288628	283506
1	6	2	1970	3176	8209	313715	288628	285892
1	6	3	2303	4288	8209	314772	288624	287338
1	7	0	1949	0	8321	335554	309424	307204
1	7	1	2020	1489	8321	338542	309424	310382
1	7	2	2220	2801	8321	340489	312344	312591

Table 16 (a) (Continued)

H	K	L	Angles (x 10^2) θ	χ	φ	Transmittances (x 10^6) TALABS	Phi Scan	TALABS (10% Measuring Error)
1	8	0	2238	0	8405	361562	328082	333104
1	8	1	2301	1312	8405	364259	332250	335979
1	8	2	2484	2499	8405	366231	335269	338182
2	0	0	452	0	0	540505	533476	508333
2	0	1	682	4837	0	540543	533476	508462
2	0	2	1120	6604	0	537943	533476	505869
2	0	3	1612	7350	0	532529	533476	500381
2	0	4	2132	7747	0	523938	533476	491638
5	0	1	1249	2422	0	540585	534560	508632
5	0	2	1538	4199	0	537949	533865	506005
5	0	3	1935	5347	0	532449	533865	500436
5	0	4	2396	6094	0	523720	533865	491564
5	1	0	1170	0	1349	532363	526116	500044
5	1	1	1279	2363	1349	532447	526116	500227
5	1	2	1563	4119	1349	529757	526116	497552
5	1	3	1955	5270	1349	524072	525130	591802
5	1	4	2413	6026	1349	514981	525130	482572
5	2	0	1263	0	2564	515677	510211	483104
5	2	1	1365	2208	2564	515820	510211	483358
5	2	2	1636	3905	2564	513124	510211	480701

Table 16 (Continued) (b) $\mu = 224\ cm^{-1}$

H	K	L	Angles (x 10^2) θ	χ	ϕ	Transmittances (x 10^6) TALABS	Phi Scan	Multiple θ-scans	TALABS (10% Measuring Error)
0	0	1	509	9000	9000	38872	48268	42788	28955
0	0	2	1022	9000	9000	42135	48268	48268	32404
0	0	3	1544	9000	9000	44583	48268	54971	35221
0	1	0	471	0	9000	56623	67284	61735	45385
0	1	1	577	6193	9000	60589	67284	62663	49352
0	1	2	1058	7507	9000	63729	67284	67284	52666
0	1	3	1569	7992	9000	66125	67284	74334	55403
0	1	4	2098	8241	9000	67788	67284	83576	57571
0	2	0	543	0	9000	78338	79911	74353	65812
0	2	1	745	4315	9000	82095	79911	77701	69578
0	2	2	1160	6193	9000	85130	86212	86212	72775
0	2	3	1641	7043	9000	87456	86212	93507	75414
0	2	4	2155	7507	9000	89131	86212	103216	77548
3	4	0	1290	0	5799	195970	216806	222956	170919
3	7	2	2321	2677	7035	152290	122159	144091	133178
8	5	1	2385	1268	3687	256134	282217	295446	226437

Table 16 (Continued) (c) $\mu = 624\ cm^{-1}$

H	K	L	Angles (x 100) θ	χ	ϕ	Transmittances (x 10^6) TALABS	Phi Scan	TALABS (10% Measuring Error)
0	0	4	2079	9000	9000	6991	5284	6545
0	1	0	271	0	9000	8460	10177	7585
0	1	1	577	6193	9000	10170	10177	9197
0	1	2	1058	7507	9000	11860	10177	10794
0	1	3	1569	7992	9000	13540	10177	12385
0	1	4	2098	8241	9000	15185	10177	13944
0	2	0	543	0	9000	16840	13419	15143
0	2	1	745	4315	9000	18502	13419	16714
0	2	2	1160	6193	9000	20154	13419	18279
0	2	3	1641	7043	9000	21781	13419	19824
0	2	4	2155	7507	9000	23380	18259	21345
0	3	0	816	0	9000	25201	18259	22685
0	3	1	964	3200	9000	26845	18259	24243
0	3	2	1314	5134	9000	28451	18259	25768

0.44¢/reflection. A very complex crystal described by 14 faces costs 1.10¢/reflection. For large data sets, the savings is considerable.

Limitations of this Method and Approaches Tried to Overcome Them

If a crystal is mounted such that its longest dimension is perpendicular to the ϕ-axis, the χ and θ dependencies become more important in calculating transmittances. If these dependencies are ignored as would be the case in this program, then the resultant transmittances can be erroneous. For example, a plate mounted with its longest direction perpendicular to the goniometer axis was examined and compared with TALABS. The complete description of the crystal orientation is given in Table 17. Assuming $\mu = 124\ cm^{-1}$, both absorption corrections were run. The results are tabulated in Table 18. The true transmittances vary with θ for a given ϕ and χ but with this program they remain fairly constant.

Several types of empirical modifications were made in an attempt to alleviate these problems. The first approach considered the path length of each reflection through the crystal to be divisible into x, y, and z components $t = t_x\vec{i} + t_y\vec{j} + t_z\vec{k}$. The vectorial sum of t_x and t_y are obtainable from the transmittance calculated from the ϕ-scan program. Since $T = e^{-\mu(t_x\vec{i} + t_y\vec{j})}$, $-\log T/\mu = t_x\vec{i} + t_y\vec{j} = 2r$, where r is the effective radius of a cylinder. The t_z component is then $r \tan\chi$. However, physically, the maximum z component is half the height of the crystal, $\ell/2$. Therefore, if $r \tan\chi > \ell/2$, then t_z would be set equal to $\ell/2$. The transmittance for each reflection is $e^{-\mu(r^2 + t_z^2)^{1/2}}$. For the test crystal oriented as given in Table 17, this approach worsened

Table 17. Flat plate test crystal

χ (in °)	ϕ (in °)	d (in cm)
0.0	90.0	0.0225
0.0	-90.0	0.0225
0.0	0.0	0.0075
0.0	180.0	0.0075
90.0	0.0	0.0025
-90.0	0.0	0.0025

Table 18. A comparison of TALABS and ϕ-scan for a flat plate crystal

			Angles (x 10^2)			Transmittances (x 10^6)	
H	K	L	ϕ	χ	ϕ	TALABS	θ-scan
0	0	1	509	9000	9000	205391	245497
0	0	2	1022	9000	9000	253915	245497
0	0	3	1544	9000	9000	302427	245497
0	0	4	2079	9000	9000	371560	245497
0	1	0	271	0	9000	158352	247242
0	1	1	577	6193	9000	207798	247242
0	1	2	1058	7507	9000	256058	247242
0	1	3	1569	7992	9000	304335	247242
0	1	4	2098	8241	9000	353474	247242
2	1	0	527	0	3096	85983	181871
2	1	1	734	4397	3096	152030	181871
2	1	2	1153	6260	3096	217520	181871
2	1	3	1636	7094	3096	280782	180668
2	1	4	2151	7547	3096	337393	181693
2	2	0	707	0	5019	128271	220719
2	2	1	873	3576	5019	185045	220719
2	2	2	1248	5523	5019	241021	220719
2	2	3	1706	6516	5019	296938	221485
2	2	4	2207	7086	5019	350571	221485
2	3	0	934	0	6094	144980	237037

the relative transmittances. For constant χ and ϕ values, the transmittance decreased with increasing θ.

The second approach was based on the observation that, for a small range in θ, the transmittance of the test crystal for a given χ and ϕ value is nearly linear in $\log(\sin^2\theta)$, or $T = m\log(\sin^2\theta)+b$, where m is the slope and b is the intercept. Using the data from two phi scans made at different θ values, the slope and intercept of the transmittance equation were calculated as a function of ϕ. The resulting transmittances increased with θ, but for $\chi \neq 90°$, non-00ℓ reflections, the relative transmittances were too large. For example, the relative transmittances of the 460, 461, 462, 463 series of reflections ranged from 0.83 to 0.90 from the ϕ-scan program whereas the range from TALABS was 0.36 to 0.80.

By comparing the relative transmittances from TALABS and the second modification, it was noted that multiplying ϕ-scan value by $(1+\sin\chi)$ would make it nearly equal to the TALABS value. The results from this third approach are quite good for the crystal described in Table 17. For instance, the relative transmittances for the 460 to 463 series of reflections ranged from 0.36 to 0.80. This program calculated this span to be 0.42 to 0.81. A differently shaped crystal was tried with this approach. It was 0.45 x 0.4 x 0.2 mm, with the 0.45 mm length parallel to the ϕ-axis. The phi scan results were quite poor. TALABS calculated the range of the 00ℓ transmittances to be 0.39 to 0.60, whereas phi scan calculated the range to be 0.22 to 0.40. From this, one may conclude that the $(1+\sin\chi)$ multiplier is very likely crystal shape dependent and is, therefore, not useful for the generalized case.

Plots of transmittances against $\log(\sin^2\theta)$ for data obtained from TALABS indicated that the slope of the line roughly increases with χ. The fourth approach scaled the calculated slope of T vs. $\log(\sin^2\theta)$ by $\sin\chi$ to accommodate the observed trends. The reflections with $\chi=0°$ have much larger relative transmittances than TALABS calculates. This occurs because the transmittance is then set equal to the intercept, which is the transmittance for $\theta=90°$. The relative transmittances for other reflections were not correct either so no further attempts were made to continue this approach.

From these attempts, it is apparent that the χ and θ dependencies of the transmittance cannot be uncoupled. Since the phi scan program effectively makes each crystal a cylinder whose height is parallel to the ϕ-axis, the transmittances for an approximation of a cylindrical crystal were examined as functions of θ, χ, and the height:radius ratio. A regular 12-sided polygon was used as input for TALABS. The radius and μ were set equal to 0.1 mm and 125 cm^{-1}, respectively, for all runs. The heights used were 0.05, 0.1, 0.2, 0.3, and 0.4 mm. A representative sample of these results is given in Table 19. The variation of the transmittances does not seem to be a simple function of χ and θ nor is it independent of the size of the crystal. It is interesting to note, however, that the χ dependence is greatest when the height is less than the diameter. For the case when h=r and $\theta = 14°$, for example, the transmittances range from 0.137874 ($\chi=0°$) to 0.202379 ($\chi=90°$), a 47% increase. The corresponding range for the crystal with h=4r is 0.137874 to 0.144113, only a 5% increase. The results are similar for any of the runs where

Table 19. TALABS calculated transmittances for a cylindrical crystal approximation

(a) ℓ = 0.05 mm, d = 0.2 mm, μ = 125 cm^{-1}

	Transmittances (x 10^6)				
χ (in °)	θ = 2°	θ = 6°	θ = 10°	θ = 14°	θ = 18°
0	132178	133207	135025	137874	146807
5	135324	139265	144689	151380	158155
10	136362	144644	153666	163761	174030
15	138171	149978	162696	176430	189463
20	140078	155307	171459	188089	204274
25	141914	160444	179704	199007	219073
30	143661	165353	187708	210022	234577
35	144952	170001	195280	220493	246146
40	146463	174355	202371	230025	257468
45	147857	178387	208936	239050	269179
50	149124	182070	214934	247310	279382
55	150253	185379	220323	254749	289187
60	151569	188292	225069	261314	297053
65	152364	190789	229139	266956	304253
70	152992	192859	232506	271632	310360
75	153450	194474	235147	275304	314833
80	153737	195638	237044	278659	318152
85	153853	196339	238186	279536	320142
90	153799	196573	238567	280066	320804

Table 19 (Continued) (b) ℓ = 0.1 mm, d = 0.2 mm, μ = 125 cm^{-1}

	Transmittances (x 10^6)				
χ (in °)	θ = 2°	θ = 6°	θ = 10°	θ = 14°	θ = 18°
0	132178	133207	135025	137874	141871
5	134754	136668	140052	144598	150930
10	135301	139189	144521	150903	157618
15	135575	141629	148646	156923	164907
20	136268	144278	152868	162692	171770
25	137019	146608	156892	167214	178952
30	137882	148974	160703	172294	186639
35	138693	151200	164090	177062	190919
40	139445	153273	167359	181355	195552
45	140133	155186	170353	185384	199815
50	140751	156912	173061	188801	204278
55	141295	158460	175470	191976	207997
60	141762	159815	177571	194736	211365
65	142149	160971	179357	197083	214221
70	142454	161922	180821	198999	216556
75	142675	162666	181961	200486	218364
80	142813	163198	182773	201543	219645
85	143516	164114	183259	202171	220405
90	142839	163624	183420	202379	220654

Table 19 (Continued) (c) ℓ = 0.2 mm, d = 0.2 mm, μ = 125 cm^{-1}

	Transmittances (x 10^6)				
χ (in °)	θ = 2°	θ = 6°	θ = 10°	θ = 14°	θ = 18°
0	132178	133207	135025	137874	144391
5	134865	135607	138414	141206	149733
10	134731	136599	139898	144451	152630
15	134748	137814	141833	147661	156125
20	135548	138892	143867	149870	159200
25	135523	139797	145385	151503	161858
30	135404	140921	147059	153709	164109
35	135527	141800	148591	155347	166265
40	135912	142732	149984	156924	170845
45	136081	143577	151062	158391	169267
50	136378	144333	152124	159674	170681
55	136637	145000	153043	160589	171163
60	136859	145576	153822	161452	171958
65	137042	146061	154463	162146	172430
70	137854	146456	154979	162683	172853
75	138314	146761	155368	163077	173130
80	137988	147544	155638	163341	173288
85	137793	147405	155796	163489	173357
90	137360	147150	155847	163535	173372

Table 19 (Continued) (d) ℓ = 0.3 mm, d = 0.2 mm, μ = 125 cm^{-1}

	Transmittances (x 10^6)				
χ (in °)	θ = 2°	θ = 6°	θ = 10°	θ = 14°	θ = 18°
0	132178	133207	135025	137874	137318
5	136440	135707	136742	140223	146400
10	134938	135622	137368	140223	145193
15	134811	135444	138028	140832	145697
20	134423	135689	137624	141230	145965
25	134926	136190	138037	141190	145665
30	134500	135920	138364	141145	145671
35	134454	136212	138615	141269	144809
40	134675	136461	138797	140823	143798
45	134690	136669	138575	140648	142806
50	134826	136504	138245	140086	141905
55	134749	136594	138197	139732	140810
60	134807	136651	138128	139362	139994
65	134833	136505	137871	139007	139221
70	134828	136477	137750	138472	138355
75	134796	136425	137949	138138	137701
80	134738	136353	138054	137873	137188
85	134891	137105	138248	138729	136854
90	134431	136167	137465	137639	136735

Table 19 (Continued) (e) ℓ = 0.4 mm, d = 0.2 mm, μ = 125 cm^{-1}

	Transmittances (x 10^6)				
χ (in °)	θ = 2°	θ = 6°	θ = 10°	θ = 14°	θ = 18°
0	132178	133207	135025	137874	141871
5	134876	135518	137188	140620	14665
10	134845	135545	138268	141051	146727
15	134758	136185	138382	142539	147719
20	134642	136334	139298	143520	148601
25	134813	136987	140116	143672	149546
30	135067	137237	140488	144434	149360
35	134867	137743	141061	144690	149596
40	135144	137822	141165	144988	148842
45	135385	138174	141504	144895	148326
50	135589	138478	141774	144983	148270
55	135755	138551	141987	144996	147547
60	136232	138730	141947	144961	147167
65	135629	139181	142019	144677	146787
70	135608	139220	142057	144525	146175
75	135217	139209	142071	144373	145768
80	134939	139151	142070	144240	145434
85	134790	139051	142474	144148	145209
90	134620	183913	142061	144113	145127

$h \geq 2r$. This indicates that the original ϕ-scan program should work quite well for crystals whose greatest dimension is parallel to the ϕ-axis and corroborates the good results from the initial testing of the program.

Suggestions for Future Work

Finding a function which describes the transmittance behavior of a cylinder without too much explicit knowledge of the size would be extremely desirable, although this might not be possible. For cases when the crystal is poorly shaped, such as when there are not discrete faces, one might try running the phi scan program and then running TALABS. The input into TALABS would be for the cylinder produced from the phi scan correction. It would be necessary to determine the effective radius of the cylinder and the height which would produce the best results first. The way to combine the results of the two programs would also have to be determined.

Another approach which might be useful is to tabulate the transmittances for $\chi = 0$ to $90°$ for a given θ value for various sizes of cylinders. The θ-dependence could be calculated separately. Data to approximate the transmittance of a cylinder with respect to θ is available in Volume II of the International Tables (49). One could then determine a transmittance to be combined with the transmittance from the phi scan program. This might require huge amounts of computer storage if it would be necessary to store data for a large number of cylinders. The computation requirements which might be necessitated to obtain good results from this type of approach could be essentially that required by TALABS.

Conclusion

This empirical absorption correction program is a very simple way to make an absorption correction. Under most circumstances, when absolute scaling is not needed, no measurements of the crystal need be made. Crystals should be mounted with their longest dimension parallel to the goniometer axis; their μ values should be less than ~400 cm^{-1}. If no reflection occurs within 10° of $\chi=\pm 90°$, this technique cannot be used on some diffractometers.

This technique has now been successfully employed in analysis of a number of structures. For example, the agreement factor for $LiZn_2Mo_3O_8$ crystals with μ = 140 cm^{-1} decreased from 6.3% to 4.9% after this absorption correction was applied. One oxygen atom in this compound which would not refine anisotropically before the correction was made refined normally afterwards (50). The agreement factor for $(C_{18}H_{36}N_2O_6K^+)_2Tl_2Te^{2-}\cdot NH_2C_2H_4NH_2$ (μ = 70.9 cm^{-1}) behaved similarly. Before the correction was made R = 11.4%; after the correction, it decreased to 9.8% (51). For some very poorly shaped crystals the ϕ-scan correction is better than the TALABS correction even in the higher ranges. An example where this occurs is YRu_4B_4, with μ = 331 cm^{-1}. The final agreement factor is 4.2% with the ϕ-scan data; with TALABS data R = 5.5% (52).

SUMMARY

The crystal and molecular structures of four interesting organometallic and organic complexes were discussed. The stabilized thioketone, $Cr(CO)_5(SCMe_2)$, has essentially octahedral coordination about the chromium atom. The Cr-C distance opposite the Me_2CS group is 1.835(12) Å, significantly shorter than the remaining Cr-C distances (averaging 1.898(2) Å). Strain in $PSN_3C_6H_{12}$ forces the nitrogens into a pyramidal configuration, with average bond angles of 109°. Each of the five-membered rings in this structure contains a carbon atom which is puckered toward the sulfur and out of the nearly planar arrays of the remaining ring atoms. The excellent consistency of non-symmetry related bond distances and angles indicates that good data can be collected using mostly unfiltered radiation. In $RhO_4N_4C_{72}BH_{76}\cdot 1.5NC_2H_3$, it has been shown that two rhodium atoms are not bridged by the large diisonitrile ligands. Each complex is a monomer, with closest Rh-Rh distances of 3.384(2) Å, a distance considered too long for significant metal-metal bonding. The molybdenum atom in $MoP_2O_{10}C_{16}H_{22}$ occupies the axial position of the six-membered ring of each of the phosphorinane ligands. This confirms that the coordination process occurs with the retention of the phosphorus' configuration.

The empirical absorption correction works very well for crystals with μ<~400 cm^{-1}, which are mounted with their longest dimension parallel to the ϕ-axis. Even when these conditions are not strictly met, this method of absorption correction can produce better results than an analytical technique when unsuitable crystal morphology prohibits accurate measurement of its size and shape.

REFERENCES

1. Gingerich, R. G. W.; Angelici, R. A. J. Organometal. Chem. 1977, 132, 377.

2. Jacobson, R. A. J. Appl. Crystallogr. 1976, 13, 2535.

3. Rohrbaugh, W. J.; Jacobson, R. A. Inorg. Chem. 1974, 13, 2535.

4. Lawton, S. L.; Jacobson, R. A. Inorg. Chem. 1968, 7, 2124.

5. Busing, W. R.; Martin, K. O.; Levy, H. A. Oak Ridge, Tennessee, Nov., 1965, AEC Report ORNL-TM-305.

6. Hubbard, C. R.; Quicksall, C. O.; Jacobson, R. A. Ames, Iowa, June, 1971, AEC Report IS-2625.

7. Hanson, H. P.; Herman, F.; Lea, J. D.; Skillman, S. Acta Crystallogr. 1960, 17, 1040.

8. Templeton, D. H. In "International Tables for X-Ray Crystallography", MacGillavry, C. H.; Riek, G. D.; Lonsdale, K., Ed.; Kynoch Press: Birmingham, England, 1962, Vol. III, Table 3.3.2.C.

9. Stewart, R. F.; Davidson, E. R.; Simpson, W. T. J. Chem. Phys. 1965, 42, 3175.

10. Johnson, C. K. Oak Ridge, Tennessee, March 1971, AEC Report ORNL-3794 (Second Revision).

11. Helland, B. J.; Quick, M. H.; Jacobson, R. A.; Angelici, R. J. J. Organometal. Chem. 1977, 95, 132.

12. Plastas, H. J.; Stewart, J. M.; Grim, S. O. Inorg. Chem. 1973, 12, 265.

13. Baker, E. N.; Reay, B. R. J. Chem. Soc. Dalton 1973, 2205.

14. Sutton, L. E. "Tables of Interatomic Distances and Configuration in Molecules and Ions, Supplement 1956-1959", The Chemical Society, Burlington House: London, 1965.

15. Cowlery, A. H. Phosphorus and Sulfur 1976, 2, 283.

16. Clardy, J. C.; Kolpa, R. L.; Verkade, J. G. Phosphorus 1974, 4, 133.

17. Romming, C.; Songstad, J. Acta Chem. Scand. Ser. A. 1978, A32(8), 689.

18. White, D. W.; Karcher, B. A.; Jacobson, R. A.; Verkade, J. G. J. Am. Chem. Soc. 1979, 101, 4921.

19. Lappert, M. F.; Pedley, J. B.; Wilkins, B. T.; Stelzer, O.; Unger, E. J. Chem. Soc. Dalton Trans. 1975, 1207.

20. Roberts, B. W.; Parrish, W. In "International Tables for X-Ray Crystallography", MacGillavry, C. H.; Riek, G. D.; Lonsdale, K., Ed.; Kynoch Press: Birmingham, England, 1962, Vol. III, Table 2.3.2A.

21. Main, P. M.; Woolfson, M. M.; Germain, G. "MULTAN: A Computer Program for the Automatic Determination of Crystal Structures", Department of Physics, University of York, York, England, 1971.

22. Cruickshank, D. W. J.; Pilling, D. E. In "Computing Methods and the Phase Problem in X-ray Crystal Analysis", Pepinsky, R.; Roberts, J. M.; Speakman, J. C., Ed.; Pergamon Press: New York, N.Y., 1961; pp 45-46.

23. Subramanian, E.; Trotter, J. J. Chem. Soc. A. 1969, 2309.

24. Rohrbaugh, W. J.; Jacobson, R. A. J. Agr. Food Chem. 1977, 25(3), 588.

25. Lapp, R. L.; Jacobson, R. A. Cryst. Struct. Comm. 1980, 9, 65.

26. Kawakami, K.; Okajima, M.; Tanaka, T. Bull. Chem. Soc. Jpn., 1978, 51, 2327.

27. Lewis, N. S.; Mann, K. R.; Gordon, J. G.; Gray, H. B. J. Am. Chem. Soc. 1976, 98, 7461.

28. Mann, K. R.; Lewis, N. S.; Miskowski, V. M.; Erwin, D. K.; Hammond, G. S.; Gray, H. B. J. Am. Chem. Soc. 1977, 99, 5525.

29. Chatt, J.; Venanzi, L. M. J. Chem. Soc. 1957, 4735.

30. Mann, K. R.; Lewis, N. S.; Williams, R. M.; Gray, H. B.; Gordon, J. G. Inorg. Chem. 1978, 17, 828.

31. Dart, J. W.; Lloyd, M. K.; McCleverty, J. A. J. Chem. Soc. Dalton 1973, 2039.

32. Yaneff, P. V.; Powell, J. J. Organometal. Chem. 1979, 179, 101.

33. Angelici, R. J.; Quick, M. H.; Kraus, G. A. Inorg. Chim. Acta 1980, 44, 2137.

34. Lapp, R. L. Ph.D. Dissertation, Iowa State University, Ames, Iowa, 1979.

35. Lapp, R. L.; Jacobson, R. A. Ames, Iowa, Aug., 1979, DOE Report IS-4708.

36. Powell, D. R.; Jacobson, R. A. Ames, Iowa, April, 1980, DOE Report IS-2155.

37. Singh, P.; Dammann, C. B.; Hodgson, D. J. Inorg. Chem. 1973, 1335.

38. Caulton, K. G.; Cotton, F. A. J. Am. Chem. Soc. 1971, 93, 1914.

39. Gaughan, A. P.; Ibers, J. A. Inorg. Chem. 1975, 14, 3073.

40. Hanson, A. W. Cryst. Struct. Comm. 1981, 10, 191.

41. Denney, D. Z.; Denney, D. B. J. Am. Chem. Soc. 1966, 88, 1830.

42. Vande Griend, L. J.; Verkade, J. G. Inorg. and Nucl. Lett. 1973, 9, 1137.

43. Ginderow, D. Acta Cryst. 1974, B30, 2798.

44. Altwood, J. L.; Darensbourg, D. J. Inorg. Chem. 1977, 16, 2314.

45. North, A. C. T.; Phillips, D. C.; Mathews, F. S. Acta Cryst. 1968, A24, 351.

46. Takusagawa, F. Department of Chemistry, Columbia University, New York, New York, private communication, 1978.

47. Alcock, A. W. presented at the International Summer School of Crystallographic Computing, Ottawa, Aug. 1969.

48. Scott, J. D. Department of Chemistry, Queen's University, Kingston, Ontario, private communication, 1971.

49. Bond, W. L. In "International Tables for X-Ray Crystallography", MacGillavry, C. H.; Riek, G. D.; Lonsdale, K., Ed.; Kynoch Press: Birmingham, England, 1962, Vol. II, Table 5.3.5A.

50. Torardi, C. C. Department of Chemistry, Iowa State University, Ames, Iowa, private communication, 1981.

51. Burns, R. C. Ames Laboratory, Iowa State University, Ames, Iowa, private communication, 1980.

52. Richardson, J. W., Jr. Department of Chemistry, Iowa State University, Ames, Iowa, private communication, 1981.

53. Wiberg, K. B.; O'Donnell, M. J. J. Am. Chem. Soc. 1979, 101, 6660.

54. Warner, P.; Chen, B. L.; Wada, E. J. Org. Chem., in press.

55. Main, P.; Lessinger, L.; Woolfson, M. M.; Germain, G.; Declerq, J. P. "MULTAN76, A System of Computer Programmes for the Automatic Solution of Crystal Structures from X-Ray Diffraction Data", University of York, York, England, 1976.

ACKNOWLEDGEMENTS

The author wishes to express thanks to the following persons:

Dr. Robert A. Jacobson, for doing well the things major professors generally do, for sharing some of his expertise in crystallography, for his absolute wizardry in Patterson analyses, and for allowing her to make mistakes and, in turn, to learn a great deal from them.

Jim Benson, the master of crystal mounting, for demonstrating this art and for his help in surviving graduate school and in data collection.

(in alphabetical order) Drs. Angelici, Shelton, Verkade, and Warner for providing interesting crystallographic problems.

Brenda Smith, a good friend as well as a good typist, for expertly preparing and proofing this thesis.

The unique individuals of X-Ray Group I for their help and friendship, especially Russ Baughman and Wayne Rohrbaugh for an introduction to the tricks of the trade, Chuck Fuller for teaching her how to fish rather than giving her a fish with respect to ORTEP, and Jim Richardson, for lengthy, bizarre discussions on absorption, from which was generally concluded, if one knows the transmittance, one knows the transmittance.

And her family for their love and support and for helping make both the good and the bad times better.

APPENDIX: SYNTHESIS OF SOME [n.1.3.1]- AND [n.1.2.1] PADDLANES

Philip Warner, Bin-Lin Chen
Catherine A. Bronski, Barbara A. Karcher
Robert A. Jacobson

From the Department of Chemistry and Ames Laboratory-USDOE
Iowa State University, Ames, Iowa 50011

Supported in part by the Petroleum Research Fund and the
U.S. Department of Energy.

The construction of paddlanes (53), i.e. tricyclic compounds in which two bridgehead carbons are linked by four non-zero bridges, is a challenging problem, particularly if all the bridges are required to be reasonably short. The approach used consisted of constructing bridgehead-bridgehead difunctionalized [m.1.1] bicyclic compounds (54), and then closing the fourth bridge. The first results of this general approach are reported here.

An examination of models indicated that a 5-7 atom bridge should be long enough to span the bridgehead positions of a bicyclo [3.1.1] heptane or bicyclo [2.1.1] hexane. The previously prepared 1a were converted into

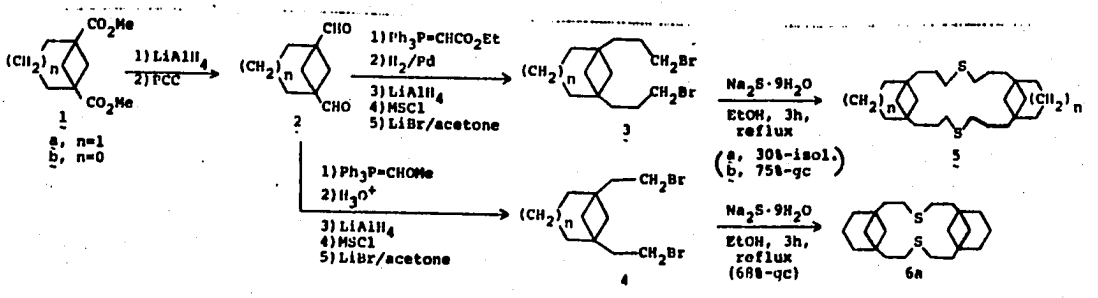

3a and 4a and 1b into 3b via the straightforward sequences shown. Treatment of 3 and 4 with Na_2S resulted in the formation of dimers 5 and 6, respectively. Their general structure was indicated by their relatively long gc retention times (OV101, 250°: 5a, 17.5 min.; 5b, 9 min.; 6a, 7 min.) and their mass spectra.

A single crystal (mp 127-8°) X-ray analysis of 5a (Figure 12) confirmed its structure. The crystals are a = 9.497(4), b = 11.003(4), c = 6.4-3(2) Å, α = 101.48(3), β = 94.95(6), and γ = 106.08(6)°, Z = 1, i.e. one dimer per cell. The inversion center is located within the center of the carbon chain ring. Using Mo K_α radiation, λ = 0.71034 Å,

Figure 12. A computer-generated drawing of $(SC_{13}H_{22})_2$

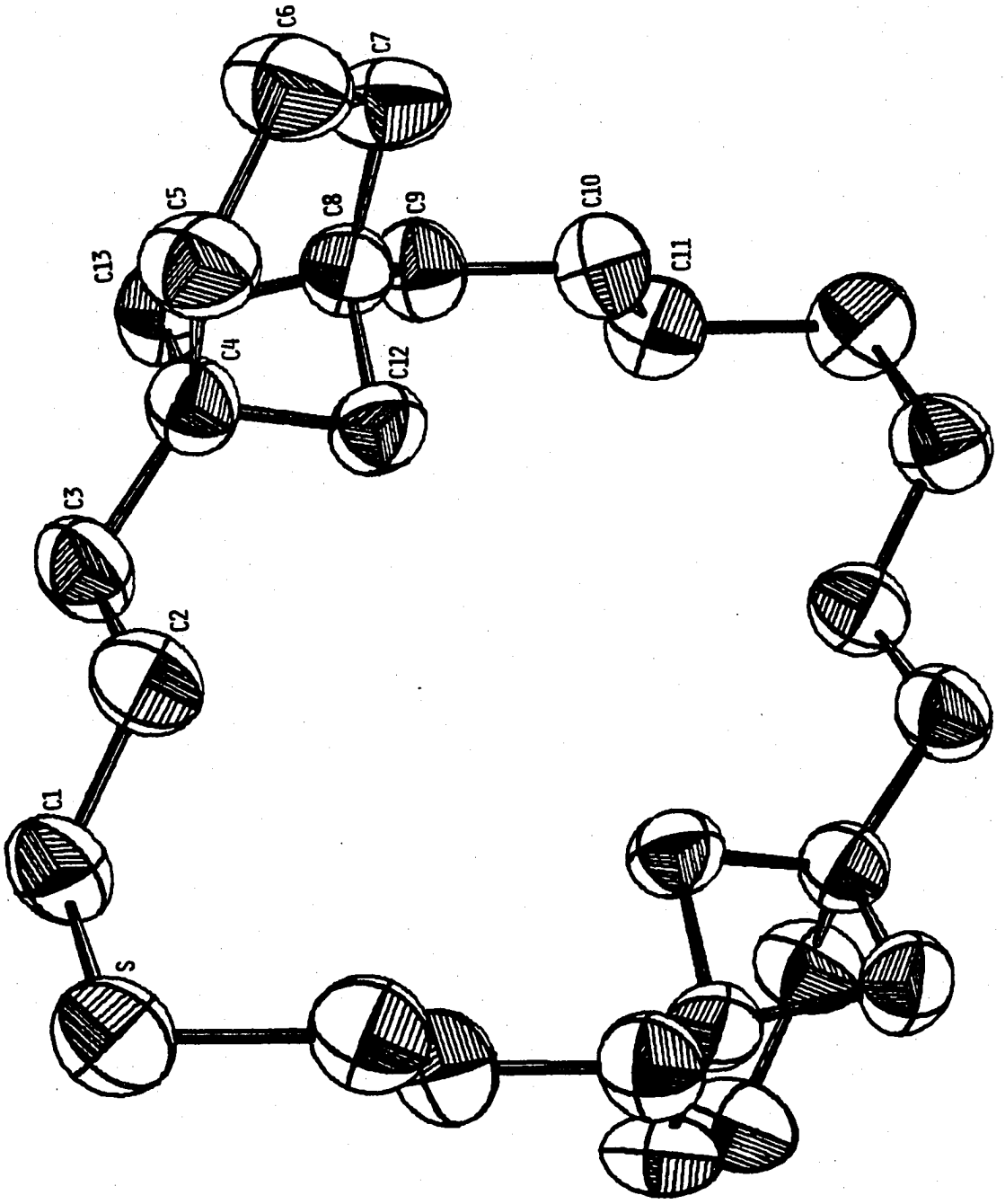
C6
C7
C5
C8
C9
C10
C13
C11
C4
C12
C3
C2
C1
S

Table 20. Final atomic positional and thermal parameters for $(PC_{13}H_{22})_2$

(a) Positional parameters (non-hydrogen atoms)

Atom	x	y	z
S	1.3229(2)	0.2829(2)	-1.0230(3)
C1	1.2683(6)	0.4286(5)	-1.0207(8)
C2	1.3036(6)	0.5265(5)	-0.8040(8)
C3	1.2613(6)	0.6471(5)	-0.8236(8)
C4	1.2594(5)	0.7353(5)	-0.6101(8)
C5	1.4099(6)	0.7855(6)	-0.4627(9)
C6	1.4128(6)	0.8883(6)	-0.2657(9)
C7	1.2650(6)	0.8990(5)	-0.2144(9)
C8	1.1379(5)	0.8280(4)	-0.3997(8)
C9	0.9910(6)	0.8513(5)	-0.3620(8)
C10	0.9278(6)	0.8001(5)	-0.1751(8)
C11	0.7629(6)	0.7760(5)	-0.1938(9)
C12	1.1393(5)	0.6856(4)	-0.4733(8)
C13	1.1943(6)	0.8486(5)	-1.6138(8)
H1-C1	1.16	0.40	-1.06
H2-C1	1.33	0.46	-1.13
H1-C2	1.25	0.48	-1.69
H2-C2	1.41	0.53	-1.77
H1-C3	1.34	0.70	-1.91
H2-C3	1.15	0.62	-1.91
H1-C5	1.47	0.80	-1.59
H2-C5	1.50	0.75	-1.42
H1-C6	1.47	0.98	-1.31
H2-C6	1.50	0.89	-1.13
H1-C7	1.22	0.86	-1.09
H2-C7	1.25	0.98	-1.19
H1-C9	1.10	0.80	-1.50
H2-C9	2.00	0.95	-1.34
H1-C10	1.97	0.73	-1.16
H2-C10	2.00	0.86	-1.03
H1-C11	0.72	0.71	0.66
H2-C11	0.73	0.86	0.78
H1-C12	1.16	0.63	-1.38
H2-C12	1.03	0.62	-1.56
H1-C13	1.27	0.94	-1.59
H2-C13	1.08	0.81	-1.72

Table 20 (Continued) (b) Thermal parameters[a]

Atom	β_{11}	β_{22}	β_{33}	β_{12}	β_{13}	β_{23}
S1	0.0216(3)	0.0141(2)	0.0500(7)	0.0083(2)	0.0160(3)	0.0035(3)
C1	0.0184(9)	0.0135(7)	0.035(2)	0.0061(6)	0.009(1)	0.0020(9)
C2	0.0175(8)	0.0120(6)	0.033(2)	0.0061(6)	0.005(1)	0.0020(8)
C3	0.1789(9)	0.0130(6)	0.029(2)	0.0063(6)	0.005(1)	0.0027(8)
C4	0.0141(7)	0.0103(5)	0.029(2)	0.0043(5)	0.0047(9)	0.0038(7)
C5	0.0122(8)	0.0156(7)	0.039(2)	0.0038(6)	0.002(1)	0.000(1)
C6	0.0141(8)	0.0151(8)	0.040(2)	0.0015(6)	0.003(1)	-0.002(1)
C7	0.0157(9)	0.0103(6)	0.040(2)	0.0034(6)	0.009(1)	-0.0028(9)
C8	0.0154(8)	0.0090(5)	0.030(2)	0.0048(5)	0.0061(9)	0.0038(7)
C9	0.0172(9)	0.0127(6)	0.035(2)	0.0068(6)	0.008(1)	0.0055(9)
C10	0.0147(8)	0.0146(7)	0.035(2)	0.0068(6)	0.006(1)	0.0063(9)
C11	0.0179(9)	0.0139(7)	0.041(2)	0.0083(6)	0.010(1)	0.0053(9)
C12	0.0141(7)	0.0088(5)	0.033(2)	0.0031(5)	0.0052(9)	0.0036(7)
C13	0.0161(8)	0.0113(6)	0.035(2)	0.0054(5)	0.007(1)	0.0064(8)

[a]The hydrogen temperature factors were set equal to 4.0Å^2.

2733 reflections were measured. There were 1765 observed reflections ($Fo>3\sigma Fo$); 1385 reflections with $2\theta < 45°$ were used in the final refinement. MULTAN76 (55) was used to locate all the non-hydrogen atoms. The final R was 8.6%; R_ω was 10.8%.

5a is formally a [17.1.3.1] paddlane, while 6a is a [13.1.3.1] paddlane. These molecules exhibit no obvious special properties; all bond distances and angles for 5a are normal. These are given in Table 21.

Experiments aimed at desulfurization and transannular closure across the big rings of 5 and 6 are underway.

Table 21. Intramolecular bond distances and angles

Distances (Å)		Angles (°)	
S-C1	1.814(7)	$\overline{C11}$[b]-S-C1	92.6(2)
$\overline{S}$[a]-C11	1.814(6)	S-C1-C2	115.5(5)
C1-C2	1.529(9)	C1-C2-C3	110.9(5)
C2-C3	1.514(9)	C2-C3-C4	114.3(5)
C3-C4	1.520(7)	C3-C4-C5	113.4(5)
C4-C5	1.539(7)	C4-C5-C6	112.8(5)
C4-C12	1.547(7)	C5-C6-C7	116.1(4)
C4-C13	1.540(9)	C6-C7-C8	113.4(4)
C5-C6	1.514(8)	C7-C8-C9	114.4(4)
C6-C7	1.500(9)	C8-C9-C10	113.7(5)
C7-C8	1.532(7)	C9-C10-C11	112.1(5)
C8-C9	1.518(8)	C10-C11-S	115.6(4)
C8-C12	1.548(6)	C3-C4-C12	118.4(4)
C8-C13	1.556(8)	C3-C4-C13	118.0(5)
C9-C10	1.526(8)	C4-C13-C8	87.4(4)
C10-C11	1.504(8)	C4-C12-C8	87.4(4)
		C12-C8-C9	117.9(4)
		C13-C8-C9	117.5(5)
		C12-C8-C13	86.4(4)
		C12-C4-C13	87.0(4)

[a] $\overline{S}$ is inversion related to S.

[b] $\overline{C11}$ is inversion related to C11.